UNIVERSITY OF CALIFORNIA, SAN DIEGO

Removal of PHLPP2 Accentuates Injury-Induced Inflammation and Cell Death of Astrocytes

A Thesis submitted in partial satisfaction of the requirements for the degree Master of Science

in

Biology

by

Lindsey Carroll Welch

Committee in charge:

Professor Nicole Purcell, Chair
Professor Brenda Bloodgood, Co-chair
Professor Ralph Greenspan

2019

The Thesis of Lindsey Carroll Welch is approved, and it is acceptable in quality and form for publication on microfilm and electronically:

Co-chair

Chair

University of California, San Diego

2019

DEDICATION

In recognition of their unwavering support, this Thesis is dedicated to my loving family.

TABLE OF CONTENTS

LIST OF ABBREVIATIONS

PHLPP	Pleckstrin Homology Leucine-rich repeat Protein Phosphatase
LPS	Lipopolysaccharide
MAP	Mitogen-Activated Protein
I/R	Ischemia/Reperfusion
ERK1/2	Extracellular signal-Regulated Kinase 1/2
ROS	Reactive Oxygen Species
CNS	Central Nervous System
GFAP	Glial Fibrillary Acidic Protein
PH	Pleckstrin Homology
RA	Ras Association
PP2C	Protein Phosphatase 2C
LRR	Leucine-Rich Repeat
BAD	Bcl-2-Associated Death promotor
GSK3	Glycogen Synthase Kinase 3
FOXO	Forkhead transcription factors
HDM2	Human Double Minute 2
TSC2	Tuberous Sclerosis Complex 2
FKBP51	FK506 Binding Protein 51
JNK	c-Jun N-terminal Kinase
NF-κB	Nuclear Factor kappa-light-chain-enhancer of activated B cells

IL-6	Interleukin 6
IL-1β	Interleukin 1 beta
IKKβ	I-kappa B Kinase beta
NLRP3	Nucleotide-binding oligomerization domain-Like Receptors Pyrin domain containing 3
COX-2	Cyclooxygenase 2
TNFα	Tumor Necrosis Factor alpha
MST1	Mammalian Sterile 20-like kinase 1
DMEM	Dulbecco's Modified Eagle Medium
FBS	Fetal Bovine Serum
DPBS	Dulbecco's Phosphate-Buffered Saline
EDTA	Ethylenediaminetetraacetic acid
OGD	Oxygen Glucose Deprivation
H_2O_2	Hydrogen peroxide
RIPA	Radioimmunoprecipitation Assay
BCA	Bicinchoninic Acid
SDS	Sodium Dodecyl Sulfate
PAGE	Polyacrylamide Gel Electrophoresis
MOPS	3-(*N*-morpholino)propanesulfonic acid
TA	Tris-Acetate
PVDF	Polyvinylidene Fluoride
TBS-T	Tris-Buffered Saline-Tween 20
BSA	Bovine Serum Albumin

DEPC	Diethyl Pyrocarbonate
dNTP	Deoxyribonucleotide Triphosphate
RT-PCR	Reverse Transcription-Polymerase Chain Reaction
qPCR	Quantitative Polymerase Chain Reaction
Ct	Comparative threshold
GAPDH	Glyceraldehyde 3-Phosphate Dehydrogenase
ELISA	Enzyme-Linked Immunosorbent Assay
ABTS	2,2'-Azino-bis(3-ethylbenzthiazoline-6-sulfonic acid)
FW	Formula Weight
SCOP	Suprachiasmatic nucleus Circadian Oscillatory Protein
SCN	Suprachiasmatic Nucleus
MCAO	Middle Cerebral Artery Occlusion

LIST OF FIGURES

LIST OF SCHEMES

ACKNOWLEDGEMENTS

I would like to acknowledge Professor Nicole Purcell for her guidance in both my research and writing process. Her support has been invaluable.

I would also like to acknowledge the members of the Purcell Laboratory, particularly Szu-Tsen Yeh and Cristina Zambrano. Their guidance has assisted me tremendously.

ABSTRACT OF THE THESIS

Removal of PHLPP2 Accentuates Injury-Induced Inflammation and Cell Death of Astrocytes

by

Lindsey Carroll Welch

Master of Science in Biology

University of California, San Diego, 2019

Professor Nicole Purcell, Chair
Professor Brenda Bloodgood, Co-chair

During an ischemic stroke, a blood clot obstructs the transport of essential nutrients to the brain, resulting in cell death (CDC 2018). The extent of injury following ischemic damage is a delicate balance between cell death and cell survival signals. Astrocytes are the most common glial cells found in the brain (Jakel and Dimou 2017). They provide metabolic and trophic support to neurons, and are pivotal responders to CNS (central nervous system) insult (Sofroniew and Vinters 2010). Survival of neurons depends on the coordinated efforts

of the neurovascular unit and health of astrocytes. PHLPP (Pleckstrin Homology domain and Leucine rich repeat Protein Phosphatase) dephosphorylates and terminates the activity of several AGC kinases that are important for controlling cell growth, proliferation, and survival (Grzechnik and Newton 2016). We have previously reported that removal of the isoform PHLPP1 increases Akt activity in astrocytes and the brain, conferring protection following ischemic injury both *in vitro* and *in vivo* (Chen et al. 2013). However, the role of the PHLPP2 isoform in the brain and in astrocytes on signaling and injury is less well understood. To study the effect of PHLPP2 removal on signaling and inflammatory responses in the brain and astrocytes, I used extracts from whole brain homogenates and primary astrocytes isolated from PHLPP2 knock-out and wild type mice. To elucidate the effect of PHLPP2 removal on inflammatory gene expression, signaling, and cell death levels under conditions that mimic ischemic injury, I performed Western blotting, mRNA analysis, and an ELISA-based cell death assay. We show that unlike removal of PHLPP1, removal of PHLPP2 is detrimental under ischemic conditions *in vitro*. Our findings suggest that therapeutics that selectively silence PHLPP1, but not PHLPP2, are needed for treatment of ischemic stroke in order to reduce brain damage.

INTRODUCTION

Astrocytes in Ischemic Stroke

According to the Centers for Disease Control and Prevention, stroke is currently the fifth leading cause of death in the United States (CDC 2019). In ischemic stroke, a blood clot obstructs a vessel that supplies blood to the brain and the affected areas become deprived of oxygen, glucose, and other essential nutrients, resulting in cell death (CDC 2018). Astrocytes are star-shaped glial cells which are highly copious in the CNS (central nervous system) and are crucially affected by ischemic stroke (Sofroniew and Vinters 2010). Their function is to provide metabolic and trophic support to neurons and modulate synaptic activity (Sofroniew and Vinters 2010). In addition to these physiological roles, astrocytes have an important role in the processes of injury and disease in the CNS. Astrocytes are pivotal responders to CNS insults under various pathological conditions and play multiple roles ranging from passive support to the regulation of inflammation during brain injuries (Sofroniew and Vinters 2010). The survival or death of astrocytes has important implications on neuronal function and survival, since astrocytes are in close contact with and provide mechanical and metabolic support to neurons.

In response to ischemic injury, neurons and glial cells of the affected area produce pro-inflammatory molecules and ROS (reactive oxygen species) (Barreto et al. 2011). This activates astrocytes to undergo reactive astrogliosis, a process in which astrocytes hypertrophy and experience cellular and molecular changes, such as increased expression of the intermediate filament protein GFAP (glial fibrillary acidic protein) and secretion of inflammatory cytokines (Kawabori and Yenari 2015; Sofroniew and Vinters 2010; Barreto et al. 2011). Injury to the CNS can elicit the activation of two different types of reactive astrocytes—one harmful (A1) and one helpful (A2) (Liddelow and Barres 2017). A1

astrocytes lose their ability to carry out their normal functions in protecting and supporting neurons, and instead contribute to CNS pathology by releasing a toxic factor that kills neurons (Liddelow and Barres 2017; Clarke et al. 2018). A2 astrocytes, on the other hand, respond to ischemia in ways that are beneficial to the CNS: they secrete neurotrophins that promote neuronal survival, upregulate thrombospondins that promote synapse repair, release antioxidants to combat ROS, clear debris and dead cells, repair the blood-brain barrier, and maintain extracellular ion levels (Liddelow and Barres 2017; Barreto et al. 2011).

In a study published by Clarke and colleagues, mouse astrocytes that had undergone normal aging appeared to take on the characteristics of A1 astrocytes (Clarke et al. 2018). The researchers reported that aged astrocytes express increased levels of GFAP and react more robustly to stimulation by the endotoxin LPS (lipopolysaccharide) as compared to controls (Clarke et al. 2018). They found that astrocytes located in regions of the brain that are most susceptible to cognitive decline, the hippocampus and the striatum, underwent more robust aging-induced astrocyte reactivity than did astrocytes of the cortex (Clarke et al. 2018). These findings are important because aging is a major risk factor for ischemic stroke. In order to fully understand these findings, it is necessary to understand the signaling pathways that occur in astrocytes during ischemia/reperfusion (I/R) injury. One key protein that is crucially involved in this signaling is Pleckstrin Homology domain and Leucine rich repeat Protein Phosphatase, commonly referred to as PHLPP (pronounced “flip”), a serine/threonine phosphatase that is ubiquitously expressed throughout the cell, with expression levels being highest in the brain (Gao et al. 2005; Chen et al. 2013).

PHLPP

In addition to having a PH (Pleckstrin Homology) domain, PHLPP also contains three other protein domains: an RA (N-terminal Ras Association) domain, a PP2C (Protein Phosphatase 2C-like) domain, and a PDZ binding domain (Grzechnik and Newton 2016) (Scheme 1). There are two isoforms of PHLPP: PHLPP1 (which is further categorized into the splice variants PHLPP1α and PHLPP1β) and PHLPP2, which has a shorter N-terminal domain (Gao et al. 2005; Grzechnik and Newton 2016). PHLPP has been demonstrated to dephosphorylate several members of the AGC kinase family to regulate a variety of cellular responses (Grzechnik and Newton 2016) (Scheme 2). One important member of the AGC family of kinases is Akt, a pro-survival serine/threonine kinase that is ubiquitously expressed throughout the cell (including astrocytes of the brain) and is comprised of three isoforms: Akt1, Akt2, and Akt3 (Mullonkal and Toledo-Pereyra 2007; Brognard et al. 2007). PHLPP has been shown to dephosphorylate the hydrophobic motif (Serine 473) of Akt, thereby partially inactivating the kinase (Gao et al. 2005). PHLPP can also directly deactivate Akt's downstream signaling kinase p70S6 kinase, which is known to promote protein translation (Liu et al. 2011; Kawasome et al. 1998). It has been found that activation of Akt promotes cell survival following cerebral ischemia through several mechanisms of action, such as phosphorylation and inhibition of the pro-death proteins BAD (Bcl-2-associated death promotor), GSK3β (glycogen synthase kinase 3 beta), and forkhead transcription factors (FOXO) (Mullonkal and Toledo-Pereyra 2007). According to a study published by Lee and colleagues, it was demonstrated that Akt activation is vital for astrocyte survival under simulated ischemia (oxygen glucose deprivation) conditions (Lee et al. 2017).

Although PHLPP1 and PHLPP2 are very similar in their structure, in cancer cells they have been found to differentially terminate Akt signaling by regulating different Akt isoforms

(Brognard et al. 2007). PHLPP1 controls the phosphorylation of the proteins HDM2 (human double minute 2) and GSK3α via dephosphorylation of the Akt2 isoform (Brognard et al. 2007). PHLPP2 controls the phosphorylation of the cell cycle inhibitor p27 via dephosphorylation of the Akt3 isoform (Brognard et al. 2007; Moller 2000). Some substrates are controlled by both PHLPP isoforms but via the dephosphorylation of distinct Akt isoforms; for example, TSC2 (tuberous sclerosis complex 2) is controlled by PHLPP1 via dephosphorylation of Akt2, and by PHLPP2 via dephosphorylation of Akt1 (Brognard et al. 2007). There are also substrates that are controlled by each PHLPP isoform and each of the three Akt isoforms, such as GSK3β and FoxO1 (Brognard et al. 2007). Although PHLPP2 has been demonstrated to dephosphorylate Akt in cancer cells, loss of PHLPP2 does not alter Akt in astrocytes basally (Chen et al. 2013). However, our laboratory has shown that removal of PHLPP1 increases phosphorylation of Akt in astrocytes (Chen et al. 2013). Thus, it was hypothesized that removal of PHLPP1 would accentuate Akt activation and protect the brain from ischemic insult.

Using PHLPP1 global knockout (KO) mice, we demonstrated that removal of PHLPP1 in primary astrocytes increased basal Akt activity, and protected the brain following ischemic damage (Chen et al. 2013). This protection was Akt-dependent since pretreatment of PHLPP1 KO mice with the Akt inhibitor triciribine caused similar ischemic injury as wild type (WT) mice (Chen et al. 2013). We also showed that in concordance with the whole brain studies, isolated PHLPP1 KO astrocytes and PHLPP1 knockdown (KD) neurons had decreased levels of apoptosis following simulated ischemia as compared to control cells (Chen et al. 2013). This study concluded that inhibition of PHLPP1 protects both astrocytes and neurons from injury in the brain caused by ischemic damage (Chen et al. 2013). The effect of PHLPP2 removal on astrocyte signaling has, however, not been examined. In one of

the few studies published to date regarding PHLPP2 in cerebral I/R injury, Wei and colleagues found that in whole rat brains *in vivo*, I/R injury induces assembly of the FKBP51-PHLPP2-Akt signaling complex, in which FKBP51 (FK506 binding protein 51) acts as a scaffolding protein that enhances PHLPP2-Akt interaction in the whole brain, thereby causing decreased Akt signaling (Wei et al. 2014). Inhibition of PHLPP2 increased pro-survival signaling through increased Akt, and decreased pro-death signaling by JNK (c-Jun N-terminal kinase) following I/R injury (Wei et al. 2014). Although the role of PHLPP2 in astrocyte signaling remains unknown, this study informs us that in whole rat brains, PHLPP2 interacts with and dephosphorylates Akt through FKBP51 binding in cerebral I/R injury *in vivo*, leading to cell death. In order to determine the role of PHLPP2 in astrocytes following I/R injury, it is critical to thoroughly understand the framework of signaling that occurs in this context as it relates to factors such as inflammation and MAP (mitogen-activated protein) kinase activation.

Inflammation and Cell Death

Brain ischemia leads to a complex chain of events that eventually results in increased brain inflammation, which causes increased death of CNS cells (Doll et al. 2014). Brain inflammation can be induced in a multitude of ways. Firstly, ischemia causes neurons and glia to depolarize; this in addition to ATP release from the damaged membranes of dead cells causes an increase in extracellular ATP levels (Doll et al. 2014). Increased extracellular ATP activates microglia to secrete ROS plus cytokines and other pro-inflammatory mediators (Doll et al. 2014). Additionally, increased neuronal death causes a decrease in cell-cell interactions with microglia, resulting in increased inflammatory signaling (Doll et al. 2014). Increased inflammatory signaling induces astrocytes to undergo reactive astrogliosis, in which they

further secrete pro-inflammatory cytokines (Kawabori and Yenari 2015; Sofroniew and Vinters 2010; Barreto et al. 2011). Hypoxia and oxidative stress that occur with ischemia lead to increased activity of NF-κB (nuclear factor kappa-light-chain-enhancer of activated B cells) and other transcription factors that increase expression of inflammatory cytokines (Doll et al. 2014). In reactive astrocytes specifically, NF-κB has been demonstrated to become activated and play an important role in reactive astrogliosis (Saggu et al. 2016). NF-κB has been known to promote the gene expression of the pro-inflammatory mediators IL6 (interleukin 6) and COX-2 (cyclooxygenase-2) (Lim et al. 2001; Libermann and Baltimore 1990). Another strong inducer of inflammation is the endotoxin LPS, which upregulates the expression of many pro-inflammatory genes such as COX-2, IL6, TNFα (tumor necrosis factor alpha), NLRP3 (Nucleotide-binding oligomerization domain-Like Receptors Pyrin domain containing 3), and IL-1β (interleukin 1beta) (Font-Nieves et al. 2012; Lamkanfi et al. 2009; Rossol et al. 2011). Because inflammation is a detrimental consequence of brain ischemia, it is necessary to understand how PHLPP2 removal affects inflammatory signaling in astrocytes in order to determine its role in I/R-induced injury.

Despite not being thoroughly studied in brain ischemia, PHLPP2 has been studied in the context of inflammation as it relates to cancer. In a study regarding gliomas (the most common tumors found in the CNS, which include astrocytomas) and colorectal cancer that was published by Agarwal and colleagues, PHLPP2 was shown to inhibit IKKβ (I-kappa B kinase beta) phosphorylation in human tumors, thereby reducing NF-κB activation (Agarwal et al. 2014; Teng et al. 2016). NF-κB is constitutively active in many cancer cells, and PHLPP2 acts as a tumor suppressor (Agarwal et al. 2014). Teng and colleagues found that PHLPP1 levels were reduced in human glioma cells as compared to control and that PHLPP1 levels were lowest in the more severe glioma tumors. Also, tumors that had PHLPP1

inhibition had the highest cytokine levels and enhanced inflammatory activity, which promotes tumor development (Teng et al. 2016). Thus, both PHLPP isoforms act as a tumor suppressor in cancer and regulate inflammation. Whether PHLPP isoforms alter inflammation following ischemic injury is not known. Reactive astrogliosis has an important role during brain injury, and the contribution of PHLPP in these processes is likely but undetermined.

One important aspect of the innate immune response that might be affected by PHLPP2 removal is the NLRP3 inflammasome (Kim et al. 2016). Mitochondrial damage leads to activation of the NLRP3 inflammasome, which then induces an inflammatory response leading to the secretion of IL-1β and IL-18 (Kim et al. 2016; He et al. 2016). IL-1β is a pro-inflammatory cytokine; its production leads to further inflammation as well as cell death (Kim et al. 2016). Activation of NF-κB is required for the activation of the NLRP3 inflammasome (Kim et al. 2016), and as mentioned above, NF-κB activation in gliomas and colorectal cancer are reduced by PHLPP2 (Agarwal et al. 2014). This raises the question as to whether PHLPP2 could have the same affect in astrocytes under ischemic damage.

Ischemia and MAPK Activation

Brain ischemia causes activation of the MAPK pathways, which have been demonstrated to regulate inflammatory responses (Irving and Bamford 2002; Wang et al. 2004). The three main MAPK pathways are ERK1/2 (extracellular signal-regulated kinase 1/2), JNK, and p38 pathways (Irving and Bamford 2002). Activation of these pathways by cellular stresses (such as cytokines and LPS) will cause phosphorylation of kinases to interact with and phosphorylate substrates in the cytosol or translocate to the nucleus where they alter the activity of transcription factors, thus leading to cellular responses (Irving and Bamford

2002; Guha et al. 2001; Saud et al. 2005). Cho and colleagues previously demonstrated that inhibition of ERK1/2 reduced brain damage in pigs that had undergone deep hypothermic circulatory arrest (Cho et al. 2004). Additionally, Aharon and colleagues found that levels of phosphorylated ERK1/2 were increased in the brains of pigs that had undergone ischemic injury, leading them to conclude that ERK1/2 inhibition might be beneficial in ameliorating I/R injury (Aharon et al. 2004). PHLPP2 has previously been demonstrated to inhibit ERK1/2 signaling (Li et al. 2014). Li and colleagues demonstrated that PHLPP2 directly dephosphorylates RAF1, which is upstream of ERK1/2, in mouse colorectal cancer cells (Li et al. 2014). They found that PHLPP2 inhibition thereby increased ERK1/2 signaling. It is possible that PHLPP2 removal might affect ERK1/2 activation in astrocytes under conditions that mimic I/R via the same mechanism that it affects ERK1/2 activation in colorectal cancer cells.

Prolonged activation of both JNK and p38 pathways have been observed in brain regions that have increased cell death following ischemic insult (Irving and Bamford 2002). Unsurprisingly, the p38 pathway is strongly activated by the inflammatory cytokines TNF-α and IL-1, both of which are upregulated in brain ischemia and are known to contribute to cell death (Irving and Bamford 2002). Several studies have investigated the effects of p38 inhibitors on cell death in brain ischemia. In a study published by Sugino and colleagues, administration of a p38 inhibitor caused decreased cell death in the CA1 region of the gerbil hippocampus following ischemia (Sugino et al. 2000). Barone and colleagues confirmed this effect by showing that administration of a more potent p38 inhibitor following brain ischemia in rats caused a decrease in infarct size and improved behavioral outcome as compared to controls (Barone et al. 2001). PHLPP2 has been studied as it relates to p38 and JNK in cancer. According to a study by Qiao and colleagues, both PHLPP isoforms were

demonstrated to indirectly activate p38 and JNK in cancer cells (Qiao et al. 2010). The researchers found that PHLPP dephosphorylates the pro-apoptotic protein Mst1 (mammalian sterile 20-like kinase 1), thereby activating it and allowing it to phosphorylate its downstream targets p38 and JNK, leading to apoptosis (Qiao et al. 2010). These findings call into question whether or not PHLPP2 could have a similar effect on p38 and JNK in astrocytes exposed to ischemic injury.

Although it had been previously discovered that PHLPP1 removal is protective during brain ischemia, the PHLPP2 isoform's role and its potentially therapeutic properties had yet to be characterized. Using primary astrocytes isolated from the brains of global PHLPP2 KO mice, I performed various *in vitro* assays in order to uncover the effect of PHLPP2 removal on inflammation and cellular signaling under conditions that mirror ischemic stroke. We found that PHLPP2 removal accentuates LPS-induced inflammatory gene expression, upregulates MAP kinase activation and NF-κB activation under conditions that simulate I/R injury, and increases simulated ischemia-induced cell death of astrocytes. Our findings suggest that PHLPP2 removal is overall detrimental in astrocytes that have been exposed to ischemic injury.

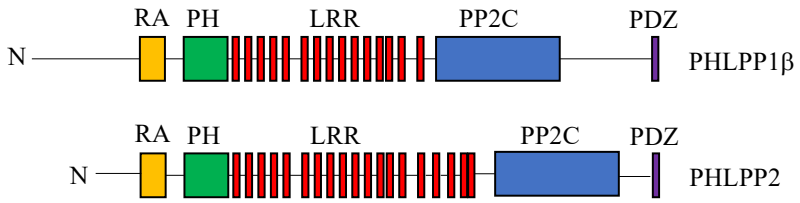

Scheme 1: PHLPP1β and PHLPP2 structure. PHLPP1β and PHLPP2 both have an N-terminal Ras Association domain, a Pleckstrin Homology domain, a Leucine-Rich Repeat region, a Protein Phosphatase 2C-like domain, and a PDZ binding domain.

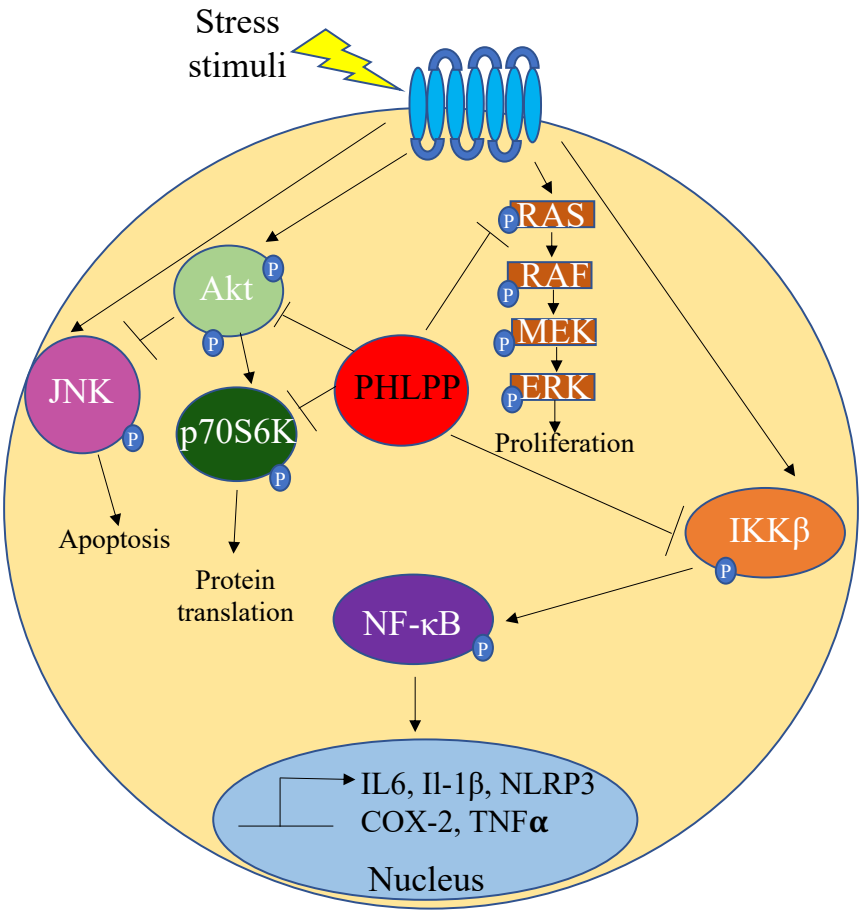

Scheme 2: PHLPP signaling. Stimulation by stress stimuli induces the RAS-RAF-MEK-ERK cascade (which leads to increased cell proliferation), IKKβ activation (which leads to activation of NF-κB and transcription of inflammatory genes such as IL6, Il-1β, NLRP3, COX-2, and TNF**α**), JNK activation (which leads to apoptosis), and Akt activation (which leads to inhibition of JNK signaling, increased p70S6 kinase activity, and increased protein translation). PHLPP inhibits RAS, IKKβ, p70S6 kinase, and Akt.

MATERIALS AND METHODS

Animals

All animal procedures were performed in accordance with the National Institutes of Health Guide for the Care and Use of Laboratory Animals and approved by the Institutional Animal Care and Use Committee of University of California, San Diego. Age matched wild-type (WT) and PHLPP2 global knockout (KO) mice were used.

Astrocyte isolation

Astrocytes were isolated from the brains of 1-3-day-old PHLPP2 WT and KO mice as previously described (Citro et al. 2007). Briefly, cerebral cortices were isolated from adherent meninges, and the tissue dissociated and trypsinized. Astrocytes were grown in T75 flasks containing Dulbecco's Modified Eagle Medium (DMEM) with 10% fetal bovine serum (FBS), antibiotics (100 units/mL penicillin and 100 μg/mL streptomycin), and glutamine at 37°C in 5% CO_2. Upon confluency, the astrocytes were shaken at 241 rpm for 18-22 hours at 37°C to remove oligodendrocytes. The astrocytes were washed with Dulbecco's phosphate-buffered saline (DPBS) two times to remove debris, and cells were incubated with 1 mL per T75 flask 0.25% Trypsin-ethylenediaminetetraacetic acid (EDTA) at 37°C in 5% CO_2 for 2-5 minutes to release cells. The Trypsin-EDTA was stopped with the addition of DMEM containing 10% FBS, antibiotics (100 units/mL penicillin and 100 μg/mL streptomycin), and glutamine. The astrocytes were split in a 1:3 ratio in T75 flasks containing DMEM with 10% FBS, antibiotics (100 units/mL penicillin and 100 μg/mL streptomycin), and glutamine, and incubated at 37°C in 5% CO_2. Experiments involving WT and KO astrocytes were plated at equal cell number and experiments performed at the second passage.

Cell culture

Following serum starvation, cells were stimulated with simulated ischemia (sI, oxygen glucose deprivation, OGD) or simulated ischemia with reperfusion (sI/R), as well as hydrogen peroxide (100 μM, H_2O_2) to mimic reactive oxygen species (ROS) formation. The endotoxin lipopolysaccharide (10 μg/mL, LPS) was used as a positive control for inflammation. OGD was carried out by combining hypoxia and hypoglycemia according to a method previously described (Chen et al. 2013). Cells were incubated with OGD medium (prepared as described in appendix) to deplete glucose from intracellular stores and extracellular space. After glucose depletion, medium was replaced with N_2-bubbled OGD medium and cultures were placed in an anaerobic chamber at 37°C with an N_2-enriched environment for either two or eighteen hours. Control cells were maintained in an incubator with 5% CO_2 at 37°C. After deprivation, cells were either harvested or incubated in culture medium under normoxic conditions (in appendix) for 30 minutes corresponding to recovery period (reperfusion).

Brain homogenization

Brains were isolated from 3-month-old PHLPP2 WT and KO mice and were snap frozen in liquid nitrogen. Tissue was homogenized in 1 mL of Western buffer (in appendix). Protein concentration was determined as described below and samples were used for Western blot analysis.

Western blot

For analysis of protein changes following stimulation, astrocytes were harvested in radioimmunoprecipitation assay (RIPA) buffer (prepared as described in the appendix). The cell lysates were water sonicated for 5 minutes and centrifuged at 14,000 rpm for 15 minutes

at 4°C, and the supernatant saved. Micro Bicinchoninic Acid (BCA) Protein Assay Kit (Thermo Scientific) was used to determine protein concentration of each sample (cell and brain extracts) according to the manufacturer's protocol. Based on the protein assay, a set protein concentration of the cell lysate was combined with 5X sodium dodecyl sulfate (SDS) (prepared as described in the appendix) and water. Samples were boiled on a 95°C heat block for 10 minutes and loaded on an SDS-polyacrylamide gel electrophoresis (PAGE) (Invitrogen NuPage) with a protein marker (BioRad). For separation of proteins, 4-12% Bis-Tris and 12% Bis-Tris Protein Gels were run in 1X 3-(*N*-morpholino)propanesulfonic acid (MOPS) buffer (prepared as described in the appendix), or 3-8% Tris-Acetate (TA) Protein Gels were run in TA buffer (prepared as described in the appendix). Gels were run at 150 V for 1-1.5 hours. The proteins were transferred to methanol-soaked polyvinylidene fluoride (PVDF) membranes (Millipore Sigma) in 1X Transfer Buffer (prepared as described in the appendix) at 100 V for 2 hours. After transfer, membranes were blocked in 5% milk/Tris-buffered saline-Tween 20 (TBS-T) (prepared as described in the appendix) for 15 minutes. The membrane was washed with 0.1% TBS-T for 5 minutes, 3 times. For analysis of protein expression, membranes were probed overnight at 4°C with primary antibodies diluted in 5% bovine serum albumin (BSA)/TBS-T (list of antibodies and dilutions are in appendix). Following primary antibody binding, membranes were washed with 0.1% TBS-T for 10 minutes, 3 times. Secondary antibodies were diluted in 5% milk/TBS-T (1:8000) and added to the membrane and incubated for 1 hour at room temperature. Following incubation with the secondary antibody, membranes were washed 3 times in 0.1% TBS-T for 5 minutes each. For visualization of proteins, blots were soaked in SuperSignal West Femto Maximum Sensitivity Substrate in a 1:1 dilution (Thermo Scientific) and exposed using a myECL Imager (Thermo Scientific). Quantitation of band intensity was analyzed using AlphaView

software.

RNA isolation/cDNA synthesis

For analysis of changes in gene expression, RNA was isolated from astrocytes using TRIzol Reagent (Thermo Scientific) according to the manufacturer's protocol. Briefly, cells were harvested in 1 mL TRIzol and cell lysates pipetted for 1 minute per sample, and incubated at room temperature for 5 minutes. Following incubation, 200 µL of chloroform was added to each sample and incubated at room temperature for 5 minutes following inversion. The lysates were centrifuged at 14,000 rpm at 4°C for 15 minutes. The supernatant was removed and added to 500 µL of isopropyl alcohol. The samples were mixed and stored overnight at -20°C to recover as much RNA as possible. Following RNA precipitation, the samples were centrifuged at 14,000 rpm at 4°C for 15 minutes. The RNA was pelleted and washed with 70% DEPC (diethyl pyrocarbonate)-treated ethanol. Following centrifugation, the RNA pellet was air-dried for 30 minutes and dissolved in 25 µL of RNAse-free sterile water. The RNA was placed on a 55°C heat block for 10 minutes to completely dissolve RNA. The concentration of RNA was determined using Gen5 Data Analysis Software (BioTek). For cDNA synthesis, 1 µg of RNA was used. cDNA master mix solution was prepared using 10X reverse transcription (RT) buffer, 25X deoxyribonucleotide triphosphate (dNTP), 10X RT primers, reverse transcriptase, and RNAse inhibitor from High-Capacity cDNA Reverse Transcription Kit (Thermo Scientific), and sterile water (as described in the appendix). For each reaction, 10 µL of cDNA master mix solution was added to the 1 µg of RNA (10 µL final volume) for a final 20 µL reaction. The samples were run on the Mastercycler Nexus PCR Machine (Eppendorf) following the RT-PCR (reverse

transcription-polymerase chain reaction) protocol (as described in the appendix). Following cDNA synthesis, the reaction was diluted by adding 20 µL of sterile water to each tube (40 µL total).

Quantitative Polymerase Chain Reaction (qPCR)

To determine the changes in gene expression following stimulation, qPCR was performed. cDNA was diluted in sterile water (1:25 dilution). For a complete list of all the primers used, refer to the appendix. For PCR, 9 µL of diluted cDNA was added to 1 µL of primer and 10 µL of qPCRBIO Probe Mix Lo-Rox (Genesee Scientific) and added to the wells of a 96-well qPCR plate. The plate was run on a 7500 fast StepOne Real-Time PCR System (Thermo Scientific). Relative quantification was analyzed using the comparative threshold cycle (Ct) method normalized to glyceraldehyde 3-phosphate dehydrogenase (GAPDH) as described previously (Schmittgen and Livak 2008).

Enzyme-Linked Immunosorbent Assay (ELISA)

DNA fragmentation indicative of apoptosis was assayed using the cell death detection ELISAPLUS (Roche Applied Science). The assay is based on a quantitative sandwich-enzyme-immunoassay using mouse monoclonal 2 antibodies directed against DNA and histones to detect cytoplasmic histone-associated-DNA fragments. For analysis of cell death following 18 hours of OGD, astrocytes were harvested in 40 µL of JNK Lysis Buffer (prepared as described in the appendix). The samples were nutated for 10 minutes at 4°C. The lysates were centrifuged at 14,000 rpm for 3 minutes at 4°C, and the supernatant transferred to a new set of tubes. Immunoreagant from the kit was prepared according to the manufacturer's instruction. To each well, 20 µL of cell lysate and 80 µL of immunoreagant

were added to a streptavidin-coated microplate (Millipore Sigma). The microplate was covered with foil and rocked for 3 hours. Micro BCA Protein Assay Kit (Thermo Scientific) was used to determine protein concentration of each sample according to the manufacturer's protocol. Following the incubation, the wells were washed three times with 200 μL incubation buffer supplied in the kit (Millipore Sigma). Following the wash, 100 μL of 2,2'-Azino-bis(3-ethylbenzthiazoline-6-sulfonic acid) (ABTS) solution (prepared according to the manufacturer's instructions) were synchronously added to the wells. Cell death levels were determined using i-control Microplate Reader Software (Tecan). The absorbance was measured at 405 nm. Measurements were normalized by dividing average read by total protein level for each sample. Folds were calculated by dividing each normalized measurement by the WT normoxic normalized measurement.

Statistical analysis

Data reflect averages ± standard error of the mean (S.E.M.) or averages ± standard deviation (S.D.). Statistical significance ($p<0.05$) was determined using Student's t-test.

RESULTS

Generation of PHLPP2 knockout mice.

Global PHLPP2 knockout mice were generated by crossing floxed PHLPP2 mice for exon 5 and 6 of the *phlpp2* gene with protamine-cre mice (Figure 1A). Protein expression of PHLPP2 and PHLPP1 was analyzed in the brains of 3-month-old wild type (WT) and PHLPP2 knockout (KO) mice (Figure 1B). It was determined that the expression of PHLPP2 protein was absent without significant alterations in the PHLPP1 isoform (Figure 1C). Our findings indicate that removal of PHLPP2 does not alter PHLPP1 and suggests that PHLPP1 and PHLPP2 may potentially have different signaling pathways.

PHLPP2 removal does not alter Akt signaling in the brain.

We have already demonstrated that removal of PHLPP1 increases Akt phosphorylation at Serine 473 and overall activity in the brain (Chen et al. 2013). However, the relationship between PHLPP2 and Akt (and its downstream targets) has not been demonstrated. Upon examination of Akt and its downstream targets in PHLPP2 KO brains, we found that PHLPP2 removal does not alter Akt signaling. Activated Akt has many downstream targets, including p70S6 kinase (which is also a direct target of PHLPP) and GSK3**α**/β (Liu et al. 2011; Mullonkal and Toledo-Pereyra 2007). p70S6 kinase regulates protein translation, and GSK3**α**/β is thought to control glycogen metabolism and gene transcription (Kawasome et al. 1998; Welsh and Proud 1993). We also looked at PHLPP's downstream target ERK1/2, a MAP kinase that promotes inflammation during brain injury, among other functions (Wang et al. 2004). Protein expression of phosphorylated Akt S473, ERK1/2, and GSK3**α**/β was analyzed in the brains of 3-month-old WT and PHLPP2 KO mice (Figure 2A). It was determined that there was no statistically significant difference in the

levels of phosphorylated Akt, ERK1/2, or GSK3α/β between WT and PHLPP2 KO brains (Figure 2A; ERK1/2 and GSK3α/β data not shown). Activation of p70S6 kinase was also analyzed in the brains of 3-month-old WT and KO mice (Figure 2B), and the levels of phosphorylated p70S6 kinase were significantly upregulated (approximately 2.1 times greater) with PHLPP2 removal compared to age-matched WT (Figure 2B). This data suggests that, unlike removal of PHLPP1, PHLPP2 removal does not alter basal Akt signaling in the mouse brain, but directly alters the phosphorylation of p70S6 kinase.

Removal of PHLPP2 does not alter PHLPP1 levels in primary mouse astrocytes.

We have already demonstrated that PHLPP2 removal does not significantly alter the levels of PHLPP1 in total brain extracts (Figure 1A), however, we wanted to determine whether removal of PHLPP2 affected PHLPP1 levels in primary astrocytes isolated from PHLPP2 KO mice. Protein expression of PHLPP2 and PHLPP1 was analyzed in isolations of WT and PHLPP2 KO mouse astrocytes (Figure 3A). As in the whole brain, removal of PHLPP2 did not significantly alter levels of PHLPP1 in isolated primary astrocytes (Figure 3B). This data further indicates that PHLPP1 does not compensate for the loss of PHLPP2 and suggests that the isoforms may potentially have different signaling pathways.

PHLPP2 removal accentuates LPS-induced inflammatory gene expression in astrocytes.

As previously discussed in the introduction, ischemic injury in the brain leads to increased inflammation and contributes to increased death of CNS cells (Doll et al. 2014). Astrocytes play a key role in the inflammatory response (Sofroniew and Vinters 2010). The effect of PHLPP2 removal on inflammatory signaling in mouse astrocytes under inflammatory conditions has not been investigated. WT and PHLPP2 KO astrocytes were

stimulated with the endotoxin lipopolysaccharide (LPS) (10 μg/mL) for six hours to induce inflammation. NLRP3 and IL-1β, which are inflammasome-dependent, and Cox2, IL-6, and TNFα, which are NF-κB-dependent, were all upregulated following LPS stimulation in the WT cells (Figure 4A and B (blue bars)) (Font-Nieves et al. 2012; Lamkanfi et al. 2009; Rossol et al. 2011). We found that removal of PHLPP2 significantly accentuated inflammatory gene expression induced by LPS compared to WT astrocytes (Figure 4A and B (orange bars)). Gene expression in LPS-stimulated PHLPP2 KO astrocytes was approximately 2.2 times greater for IL-1β, 1.7 times greater for TNFα, 2.0 times greater for NLRP3, 1.9 times greater for Cox2, and 1.3 times greater for IL-6 as compared to in the LPS-stimulated WT astrocytes (Figure 4A and B). Our findings suggest that PHLPP2 removal accentuates the inflammatory response and might be detrimental following brain injury.

PHLPP2 removal alters signaling in mouse astrocytes following simulated I/R.

Our previous experiment indicated that PHLPP2 removal accentuates inflammatory gene expression during inflammation in mouse astrocytes (Figure 4A and B). Using an *in vitro* model of stroke to induce ischemic injury, the role of PHLPP2 removal on signaling pathways that regulate inflammation and cell survival and death were investigated. The phosphorylation of Akt S473, NF-κB (p65), p38, ERK1/2, and JNK was analyzed in WT and PHLPP2 KO astrocytes that had undergone simulated ischemia (oxygen-glucose deprivation) for 2 hours and reperfusion for 30 minutes (Figure 5). Phosphorylation of each of the aforementioned proteins increased in the WT cells after reperfusion as compared to after ischemia alone (except for p38 phosphorylation, which did not change). The increased phosphorylation did not reach statistical significance for any of the proteins except for JNK. It was determined that PHLPP2 removal led to upregulation of phosphorylation of each of the

aforementioned proteins under both ischemia alone and following reperfusion as compared to in the WT astrocytes. This upregulation reached statistically significant levels under ischemia alone for Akt (approximately 8.4 times greater than WT), NF-κB (approximately 1.9 times greater than WT), ERK1/2 (approximately 1.9 times greater than WT), and JNK (approximately 2.6 times greater than WT), and under ischemia with reperfusion for Akt (approximately 3.1 times greater than WT). After reperfusion, levels of phosphorylated Akt, JNK, and ERK1/2 remained significantly upregulated in the PHLPP2 KO astrocytes as compared to WT astrocytes under ischemia alone. It should be noted that under basal conditions, PHLPP2 KO astrocytes did not alter levels of Akt activation. Therefore, PHLPP2 removal appears to only potentiate Akt activation under ischemic conditions. Our findings indicate that PHLPP2 removal accentuates MAP kinase and NF-κB signaling in astrocytes exposed to simulated ischemia, suggesting that PHLPP2 removal might cause increased inflammation and cell death in astrocytes that have been exposed to I/R.

PHLPP2 removal alters ERK1/2, but not Akt S473, phosphorylation following ROS stimulation of astrocytes.

Hydrogen peroxide (H_2O_2) is a reactive oxygen species (ROS) that is released during reperfusion injury (Granger and Kvietys 2015). To further investigate the effect of PHLPP2 removal under conditions that mimic ROS formation, WT and PHLPP2 KO astrocytes were stimulated with H_2O_2 (100 μM) for various times. Following stimulation, we found that hydrogen peroxide increased phosphorylation of both Akt S473 and ERK1/2 in the WT cells. PHLPP2 removal did not significantly alter levels of phosphorylated Akt S473 compared to WT, but did significantly accentuate phosphorylation of ERK1/2 compared to WT (Figure 6A and B). Upregulation of phosphorylated ERK1/2 reached statistical significance following 5

(approximately 1.7 times greater than WT), 10 (approximately 2.0 times greater than WT), and 30 (approximately 1.9 times greater than WT) minutes of H_2O_2 stimulation. This indicates that PHLPP2 removal accentuates ERK1/2 signaling in astrocytes exposed to ROS stimulation, suggesting that PHLPP2 removal might alter inflammatory or survival responses following reperfusion injury. We also found that PHLPP2 removal upregulated phosphorylation of p70S6 kinase (Figure 6C) basally and following stimulation with hydrogen peroxide. This finding suggests that p70S6 kinase is a direct target of PHLPP2 in both the brain (Figure 2B) and in primary astrocytes, suggesting that PHLPP2 removal might alter protein translation following injury.

PHLPP2 removal accentuates ischemic cell death of mouse astrocytes.

Our previous experiments have indicated that PHLPP2 removal accentuates pro-death MAP kinase and pro-inflammatory signaling in astrocytes under conditions that mimic ischemia and/or reperfusion injury *in vitro*. To further investigate PHLPP2 removal as it relates to cell survival under conditions that simulate ischemic injury, WT and PHLPP2 KO astrocytes were subjected to 18 hours of oxygen-glucose deprivation. Following ischemic injury, we determined that cell death levels were increased in the PHLPP2 KO astrocytes as compared to WT (approximately 2.1 times greater than WT). Although the data did not reach statistical significance, it is trending towards significance (Figure 7). This result, in conjunction with our other findings, supports the notion that PHLPP2 removal is detrimental to astrocytes that are exposed to ischemic injury.

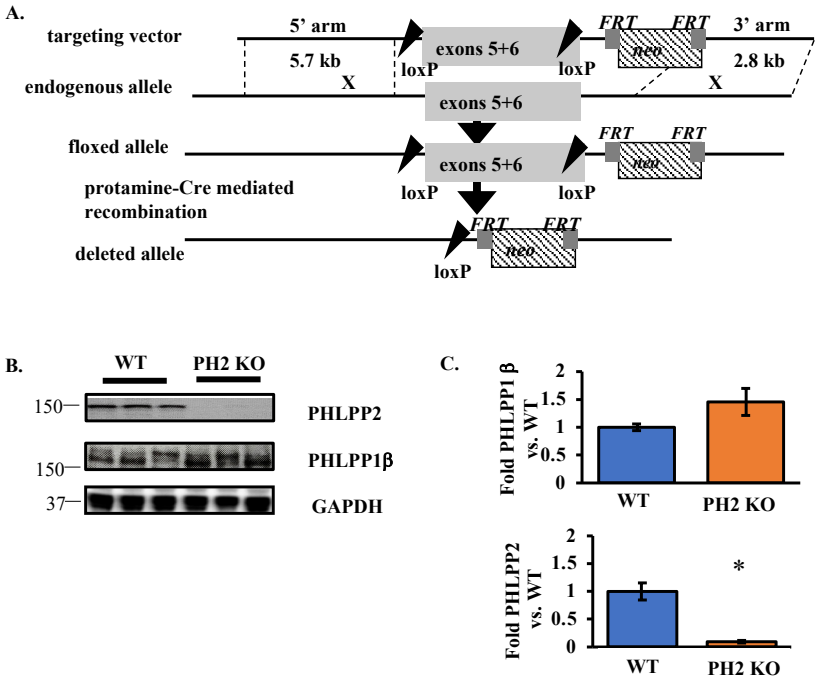

Figure 1: Targeted disruption of the PHLPP2 gene. (A) Schematic representation of the PHLPP2 genomic loci, targeting constructs, and the recombined loci deleted for the indicated exons. **(B)** Western blot analysis and **(C)** quantitation of whole brain extracts from 3-month-old PHLPP2 knockout (PH2 KO) (orange bars) and wild type (WT) (blue bars) mice for PHLPP1β and PHLPP2 expression. GAPDH is the loading control. (*$p<0.05$ vs. WT; means ± S.E.M.; n=3 animals.)

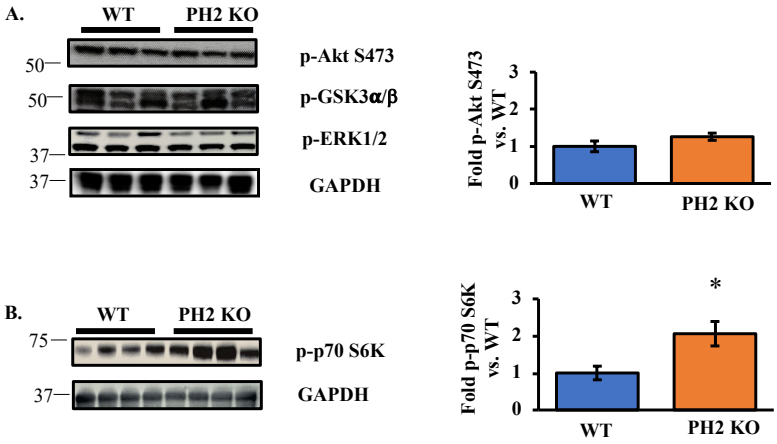

Figure 2: PHLPP2 removal does not affect Akt signaling in the brains of 3-month-old mice. **(A)** Western blot analysis of whole brain extracts from 3-month-old PH2 KO (orange bar) and WT (blue bar) mice for phosphorylated Akt Serine 473, GSK3α/β, and ERK1/2 expression, and quantitation of phosphorylated Akt Serine 473 data. GAPDH is the loading control. **(B)** Western blot analysis and quantitation of whole brain extracts from 3-month-old PH2 KO (orange bar) and WT (blue bar) mice for phosphorylated p70S6 kinase expression. GAPDH is the loading control. (*p<0.05 vs. WT; means ± S.E.M.; n=3 animals for phosphorylated Akt Serine 473; n=4 animals for phosphorylated p70 S6K.)

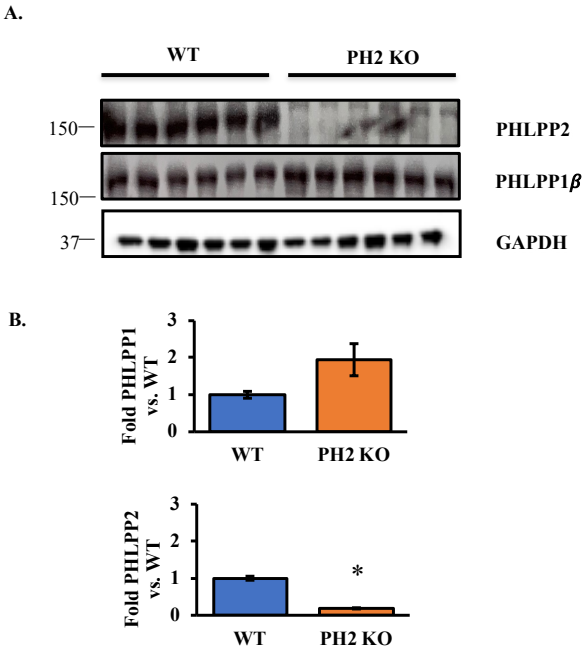

Figure 3: PHLPP2 removal does not alter PHLPP1β levels in mouse astrocytes. **(A)** Western blot analysis and **(B)** quantitation of astrocytes from WT and PH2 KO mice for PHLPP2 and PHLPP1β expression. GAPDH is the loading control. (*p<0.05 vs. WT; means ± S.E.M.; n=6).

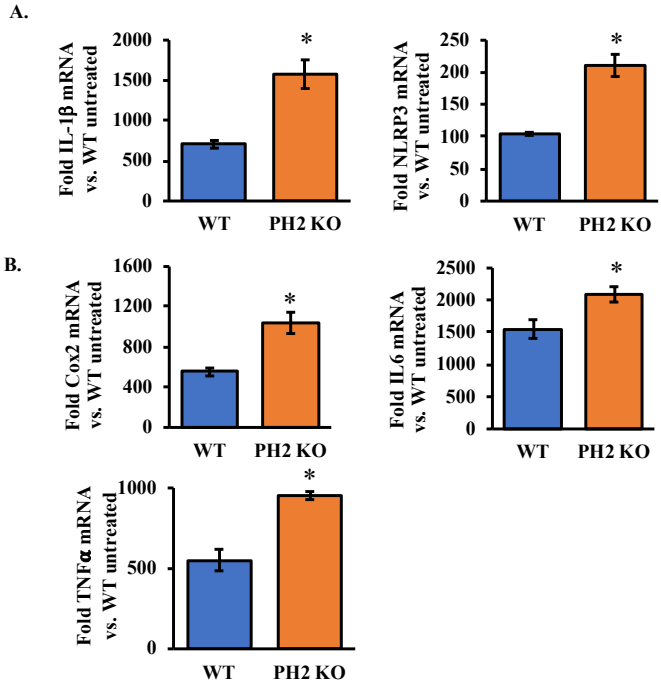

Figure 4: PHLPP2 removal accentuates LPS-induced inflammatory gene expression in mouse astrocytes. WT (blue bars) and PH2 KO (orange bars) mouse astrocytes were stimulated with 10 µg/mL LPS for 6 hours. Graphs represent fold changes in mRNA expression of **(A)** NLRP3 and IL-1β, which are inflammasome-dependent, and **(B)** TNF**α**, Cox2, and IL-6, which are NF-κB-dependent, vs. WT untreated. (*$p<0.05$ vs. WT + LPS; means ± S.E.M.; n=3.)

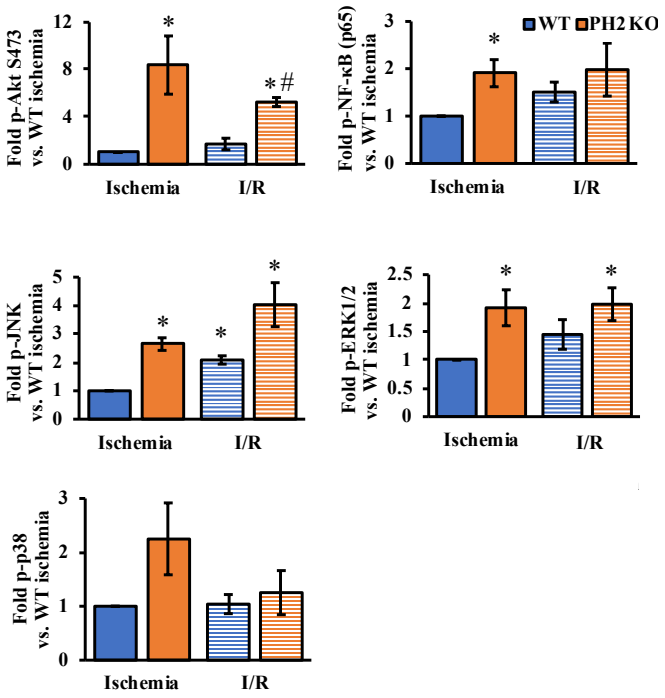

Figure 5: PHLPP2 removal alters signaling in mouse astrocytes following simulated I/R. WT (blue bars) and PH2 KO (orange bars) mouse astrocytes were subjected to 2 hours of simulated ischemia or 2 hours of simulated ischemia with 30 minutes of reperfusion. Graphs represent fold changes in phosphorylated Akt Serine 473, p38, JNK, ERK1/2, and p65 expression vs. WT ischemia. (*$p<0.05$ vs. WT ischemia; #$p<0.05$ vs. WT ischemia + 30' reperfusion; n=3 for phosphorylated Akt Serine 473, p38, ERK1/2, and p65; n=2 for phosphorylated JNK; means ± S.E.M. for phosphorylated Akt Serine 473, p38, ERK1/2, and p65; mean ± S.D. for phosphorylated JNK.)

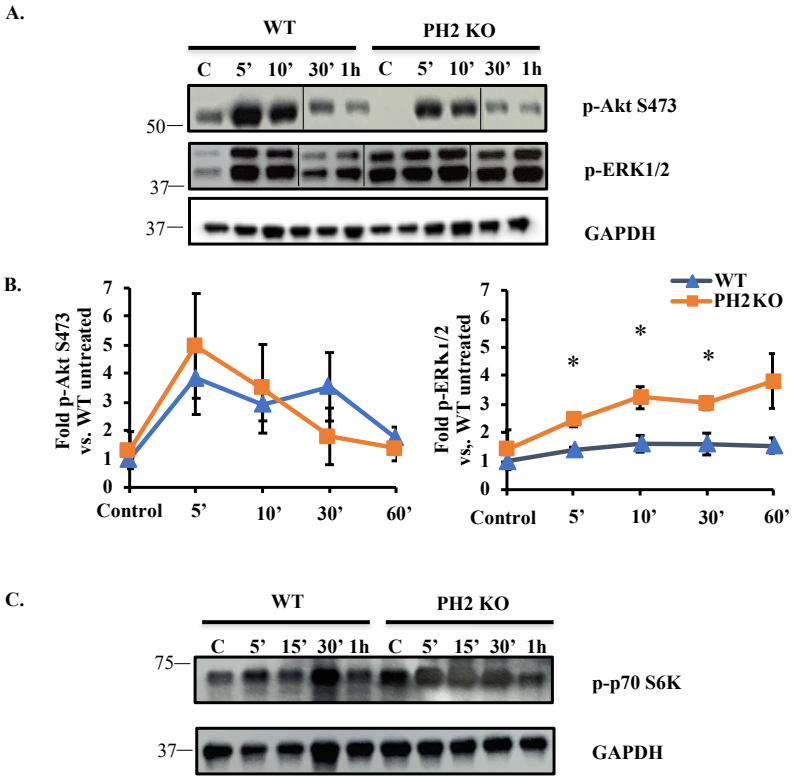

Figure 6: PHLPP2 removal alters ERK1/2 and p70 S6K, but not Akt, phosphorylation following ROS stimulation of primary astrocytes. (A) Western blot analysis and **(B)** quantitation of extracts from PH2 KO (orange lines) and WT (blue lines) mouse astrocytes following 5, 10, 30, or 60 minutes of hydrogen peroxide (100 µM) stimulation for phosphorylated Akt Serine 473 and ERK1/2 expression vs. WT untreated. GAPDH is the loading control. The lines in **(A)** indicate removal of the 15 minute time points for both phosphorylated Akt Serine 473 and ERK1/2, and to correct for consistent loading order for phosphorylated ERK1/2. **(C)** Western blot analysis of extracts from PH2 KO and WT mouse astrocytes following 5, 15, 30, or 60 minutes of hydrogen peroxide (100 µM) stimulation for phosphorylated p70 S6K expression. GAPDH is the loading control. (*p<0.05 vs. WT; means ± S.E.M.; n=5 for phosphorylated Akt Serine 473 for all time points except for the 10 minute time point which was based on an n=4; n=3 for phosphorylated ERK1/2.)

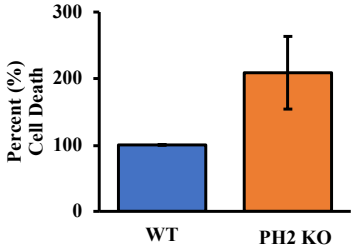

Figure 7: PHLPP2 removal increases cell death in mouse astrocytes following simulated ischemia. WT (blue bar) and PH2 KO (orange bar) mouse astrocytes were subjected to 18 hours of simulated ischemia. Graphs represent percent cell death. (*p<0.05 vs. WT; means ± S.E.M.; n=3.)

DISCUSSION

PHLPP1 and PHLPP2 are serine/threonine phosphatases that are similar in structure and are both ubiquitously expressed throughout the cell (Gao et al. 2005; Grzechnik and Newton 2016). The PHLPP phosphatases have been demonstrated to dephosphorylate several members of the AGC kinase family, including the pro-survival serine/threonine kinase Akt, in order to regulate a variety of cellular responses (Grzechnik and Newton 2016; Mullonkal and Toledo-Pereyra 2009; Brognard et al. 2007). Our laboratory previously generated global PHLPP1 KO mice via disruption of the *PHLPP1* gene (Chen et al. 2013). Using PHLPP1 KO mice, we demonstrated that removal of PHLPP1 increases Akt phosphorylation, and decreases cell death of astrocytes under simulated ischemia (Chen et al. 2013). The same result was also found using neurons with PHLPP1 knock-down (Chen et al. 2013). Additionally, PHLPP1 KO mice that had undergone middle cerebral artery occlusion (MCAO), a model of stroke, displayed increased Akt phosphorylation and a decreased infarct volume compared to WT mice (Chen et al. 2013). The decreased injury was Akt dependent since pretreatment with an Akt inhibitor in PHLPP1 KO mice prevented protection (Chen et al. 2013). This study informed us that PHLPP1 removal leads to increased Akt activity and is therefore protective to astrocytes, hippocampal neurons, and the brain following ischemic damage. However, the effect of PHLPP2 removal on signaling in the brain and its effect on astrocytes under ischemic conditions has not been previously demonstrated. Thus, we generated global PHLPP2 KO mice via disruption of the *PHLPP2* gene in order to investigate these questions. Here we demonstrate that removal of PHLPP2 does not alter Akt signaling in the brain basally, accentuates inflammatory signaling in astrocytes, and is detrimental under conditions that mimic I/R injury.

In the present study, we investigated the effect of removal of the PHLPP2 isoform on PHLPP1 expression and downstream signaling pathways targeted by the phosphatase in the brain of 3-month-old mice under basal conditions. Although I found that PHLPP2 removal does not affect PHLPP1 levels in the brain or in astrocytes basally, further studies are needed to investigate whether PHLPP2 removal alters PHLPP1 levels in the brain following I/R injury, or with aging (because aging is a major risk factor for brain ischemia). Alterations in PHLPP1 levels could affect pro-survival Akt phosphorylation since PHLPP1 dephosphorylates Akt in the brain under simulated I/R injury (Chen et al. 2013); thus, it would be beneficial to investigate whether or not PHLPP1 levels are affected by PHLPP2 removal in the brain under simulated I/R or with aging. Preliminary data from our laboratory not represented here suggests that with aging (24 months), WT mice exhibit decreased Akt phosphorylation and increased PHLPP1 with a corresponding decrease in PHLPP2 levels in the brain. Overall changes in PHLPP protein expression may alter the susceptibility of the brain to ischemic damage.

Although the two isoforms are similar in structure, PHLPP1 and PHLPP2 are not identical (Grzechnik and Newton 2016). PHLPP2 has a shorter N-terminal domain and a longer leucine-rich repeat region as compared to PHLPP1 (Grzechnik and Newton 2016). Additionally, according to Brognard and colleagues, differences in PHLPP isoform signaling could be attributed to binding specificity or differences in regulatory domains of the two isoforms (which limit substrate phosphorylation) (Brognard et al. 2007). Our previous study found that PHLPP1 removal from the whole brain under basal conditions resulted in significantly increased Akt kinase activity, as measured by increased phosphorylation of Akt's downstream target GSK3 (Chen et al. 2013). Other studies have shown that PHLPP2 targets Akt in cancer cells and *in vivo* in the whole rat brain under I/R (Brognard et al. 2007;

Wei et al. 2014; Li et al. 2014). In our present study, we found that PHLPP2 removal in the whole brain basally does not affect Akt phosphorylation or activity (as measured by phosphorylation of GSK3α/β). The reason as to why PHLPP2 targets certain substrates in some cell types or tissues but not others is currently unknown and is an avenue for future research. While PHLPP2 removal does not alter basal changes in Akt activity in the brain, it does not rule out the possibility that it may alter Akt and its downstream targets under ischemic or stress conditions. We can conclude from the present study that not only does PHLPP1 not compensate for the loss of PHLPP2, but PHLPP1 and PHLPP2 do not appear to have identical signaling pathways.

PHLPP1β, which is also known as SCOP (suprachiasmatic nucleus circadian oscillatory protein) because its expression oscillates in a circadian pattern in the hypothalamic suprachiasmatic nucleus (SCN), has been demonstrated to bind to and inhibit K-Ras, which is an upstream activator of ERK1/2, in certain key parts of the brain (Shimizu et al. 2010). ERK1/2 has been demonstrated to play a vital role in memory consolidation and cell proliferation; therefore, PHLPP1β plays a role in memory consolidation and cell proliferation as well (Shimizu et al. 2010). ERK1/2 has also previously been demonstrated in cancer cells to be a target of PHLPP2 (Li et al. 2014). In the present study, we found that PHLPP2 removal does not affect ERK1/2 signaling in the whole brain under basal conditions. As mentioned previously, PHLPP1 and PHLPP2 do not have identical signaling pathways, and it is possible for PHLPP2 to target some substrates in certain cell types or tissues but not in others. It had been previously demonstrated by Liu and colleagues that p70S6 kinase is a direct target of PHLPP independent of Akt (Liu et al. 2011). In agreement with these findings, we found that levels of phosphorylated p70S6 kinase, which upregulates protein translation (Kawasome et al. 1998), were significantly upregulated upon removal of PHLPP2

in both 3-month-old mouse brains and primary astrocytes without altering Akt. Our finding supports the notion that PHLPP2 directly targets p70S6 kinase in both astrocytes and in the brain, suggesting that removal of PHLPP2 may increase protein translation important for cell growth and proliferation. Future studies are needed to determine whether this pathway is involved in PHLPP2-mediated responses to injury in the brain.

In the present study, we only investigated the effect of PHLPP2 removal on the brain under basal conditions, but not under conditions of stress. To gain more knowledge about the effect of PHLPP2 removal on ischemic injury, it would be beneficial to study these pathways under *in vivo* conditions that mimic stroke, such as MCAO. We also only investigated PHLPP2 removal as it relates to Akt, ERK1/2, and p70S6 kinase signaling, but not as it relates to any of the other pathways that PHLPP is known to target. Other pathways that are relevant to ischemic injury and inflammation in the brain include the NF-κB and other MAP kinase pathways (i.e. p38 and JNK) (Irving and Bamford 2002; Wang et al. 2004; Doll et al. 2014). As previously discussed, these pathways are involved in inflammation, which can promote cell death (Irving and Bamford 2002; Wang et al. 2004; Doll et al. 2014). Therefore, it would be important to determine the effect of PHLPP2 removal on these pathways in the brain basally and following injury. Although our findings suggest that PHLPP1 and PHLPP2 may have different signaling pathways in the brain, it is important to investigate the effect of PHLPP2 removal on signaling in cells, including astrocytes.

Ischemic injury in the brain leads to increased inflammation and cytokine release, which overall contributes to increased cell death (Doll et al. 2014). Upon ischemic injury, neurons and glial cells produce ROS, pro-inflammatory cytokines, and other mediators of inflammation (Barreto et al. 2011). This induces astrocytes to undergo reactive astrogliosis, in which they further secrete pro-inflammatory cytokines (Kawabori and Yenari 2015;

Sofroniew and Vinters 2010; Barreto et al. 2011). Additionally, ischemic injury leads to increased activation of NF-κB and the MAP kinases, which all regulate the inflammatory response (Irving and Bamford 2002; Wang et al. 2004; Doll et al. 2014). Specifically, NF-κB is activated in reactive astrocytes and plays an important role in reactive astrogliosis (Saggu et al. 2016). According to a study by Saggu and colleagues, astrocyte-specific knock-down of NF-κB in mouse reactive astrocytes from white matter of the brain reduced levels of reactive astrogliosis and was protective of neurons and the brain (Saggu et al. 2016). Because increased inflammation occurs as a result of ischemic injury and it has been known to contribute to increased cell death (Doll et al. 2014), we investigated the effect of PHLPP2 removal on inflammatory signaling in astrocytes under conditions that mimic I/R injury. The endotoxin LPS was used as a positive control for inflammation in this study because it is a strong inducer of inflammation and upregulates the expression of many pro-inflammatory genes including COX-2, IL6, TNF**α**, and IL-1β (Font-Nieves et al. 2012; Lamkanfi et al. 2009; Rossol et al. 2011).

In a prior study, Agarwal and colleagues demonstrated that PHLPP2 inactivates IKK*β* kinase, thereby repressing activation of NF-κB, in human gliomas (Agarwal et al. 2014). In the present study, we found that PHLPP2 removal accentuates LPS-induced inflammatory gene expression of the NF-κB-dependent genes TNF**α**, Cox2, and IL-6. This result—in conjunction with our finding that PHLPP2 removal upregulates NF-κB (p65) phosphorylation in astrocytes exposed to simulated ischemia—supports the notion that PHLPP2 regulates NF-κB in an inhibitory manner. Even though the study published by Agarwal and colleagues was on human gliomas rather than primary mouse astrocytes exposed to simulated ischemia or LPS, their proposed mechanism offers an explanation as to why NF-κB was activated and downstream gene expression was significantly increased upon loss of PHLPP2 (Agarwal et al.

2014). Future studies are needed to investigate whether PHLPP2 directly targets NF-κB or its upstream kinase IKKβ in astrocytes during simulated ischemia or following LPS stimulation. To further investigate NF-κB activity, use of the NF-κB luciferase reporter in astrocytes as well as nuclear translocation of p65 by immunocytochemistry can be used under conditions that mimic I/R. Also, an NF-κB inhibitor can be used in culture to determine whether NF-κB activity is necessary for the increased inflammatory response in PHLPP2 KO astrocytes.

The NLRP3 inflammasome is an important part of the innate immune response that promotes inflammation via inducing the secretion of IL-1β and IL-18 (Kim et al. 2016; He et al. 2016). IL-1β is a pro-inflammatory cytokine; its production leads to further inflammation as well as cell death (Kim et al. 2016). Activation of NF-κB is necessary for LPS-induced gene expression of NLRP3 (Qiao et al. 2012). In addition to TNFα, Cox2, and IL-6 gene expression, we also found that gene expression of the inflammasome-dependent genes NLRP3 and IL-1β are upregulated with PHLPP2 removal in astrocytes following LPS stimulation. The upregulation of NLRP3 and IL-1β gene expression observed with PHLPP2 removal can also be explained by the mechanism related to PHLPP2 and NF-κB mentioned above. While our data suggests alterations in genes involved in the inflammasome, the protein expression of NLRP3 as well as the inflammatory cytokines needs to be determined by western blotting following simulated I/R in WT and KO astrocytes to confirm our findings. Also, activity of caspase 1, which is recruited by NLRP3 and cleaves pro-IL-1β into its mature form (Qiao et al. 2012), needs to be examined in the astrocytes following simulated I/R or LPS stimulation. Taken together, our findings suggest that removal of PHLPP2 may alter multiple pathways to induce pro-inflammatory gene expression and therefore may be detrimental to astrocytes under ischemic conditions or endotoxin exposure.

Activation of the MAP kinases—JNK, ERK1/2, and p38—has been suggested to be induced by inflammation and brain ischemia to promote pro-death signaling (Irving and Bamford 2002; Szydlowska et al. 2010). ROS levels majorly increase at reperfusion, and JNK has been demonstrated to be activated by ROS (Shi et al. 2014; Granger and Kvietys 2015). It has been demonstrated in cancer that PHLPP directly dephosphorylates and therefore activates the protein Mst1, which plays an important role in apoptosis through its downstream targets JNK and p38 (Qiao et al. 2010). It has also been previously demonstrated in mouse epidermal cells that loss of PHLPP2 leads to increased activation of the transcription factor c-Jun, which is one of the most notable transcription factors activated by JNK, in a JNK-independent manner (Zhu et al. 2014). In our model of simulated I/R, we found that JNK activation was significantly increased at ischemia with PHLPP2 removal. We also found that in the WT astrocytes, JNK activation was significantly increased with reperfusion as compared to ischemia alone, possibly due to increased ROS at reperfusion. JNK activation was accentuated by PHLPP2 removal and appeared to act synergistically; JNK activation was at its highest with PHLPP2 removal at reperfusion. Although Zhu and colleagues characterized the observed upregulation of c-Jun activation with PHLPP2 loss as being JNK-independent in epidermal cells (Zhu et al. 2014), it is still possible that PHLPP2 loss could lead to upregulation of c-Jun phosphorylation in a JNK-dependent manner in astrocytes following simulated I/R. Future studies should investigate c-Jun phosphorylation in PHLPP2 KO astrocytes that have been treated with a JNK inhibitor under I/R conditions. Although our finding does not appear to agree with the previous finding regarding PHLPP and Mst1, future studies could investigate Mst1 levels in PHLPP2 KO astrocytes under simulated I/R to gain more information. Since JNK activation has been suggested to promote cell death in the brain following cerebral ischemia (Irving and Bamford 2002), our findings suggest that PHLPP2

removal is likely to be detrimental to astrocytes under simulated I/R in a JNK-dependent manner.

Li and colleagues have demonstrated that PHLPP2 inhibition increased ERK1/2 signaling in mouse colorectal cancer cells (Li et al. 2014). They proposed that PHLPP2 directly dephosphorylates RAF1, which is upstream of ERK1/2 (Li et al. 2014). The Ras Association domain of PHLPP has been shown to be involved in regulation of ERK1/2 signaling (Shimizu et al. 2010). We found that ERK1/2 phosphorylation was significantly increased following simulated ischemia with PHLPP2 removal as compared to WT astrocytes. Additionally, under ROS stimulation, we found that ERK1/2 activation was potentiated in PHLPP2 KO astrocytes compared to WT. While we did not detect changes in ERK1/2 activation basally in the brain with PHLPP2 removal, it is possible that following simulated I/R, removal of PHLPP2 accentuates ERK1/2 activation through increased phosphorylation of its upstream kinase RAF1 in astrocytes. Further studies are needed to look at alterations in upstream signaling of ERK1/2 as well as its kinase activity following simulated I/R in WT and KO astrocytes. Like JNK signaling, activation of ERK1/2 signaling pathway has been demonstrated to promote cell death and be involved in inflammation (Irving and Bamford 2002; Szydlowska et al. 2010; Wang et al. 2004). Thus, the observation that PHLPP2 removal causes increased ERK1/2 phosphorylation in astrocytes under conditions that mimic I/R further implies that PHLPP2 removal is overall detrimental in cerebral I/R. Further studies are needed to delineate the contribution of the two signaling pathways in ischemic injury. Through the use of ERK and JNK inhibitors, we can determine whether the pathways work synergistically or in parallel following simulated I/R with PHLPP2 removal.

Like JNK and ERK1/2, p38 has also been described as being pro-death and involved in inflammation in brain I/R injury (Irving and Bamford 2002; Szydlowska et al. 2010). As

previously mentioned, it is a known downstream target of PHLPP via PHLPP's activation of Mst1, which then activates p38 (Qiao et al. 2010). Because we saw no significant change in p38 phosphorylation with PHLPP2 removal under simulated I/R, our preliminary data suggests that PHLPP2 removal may not alter p38 in astrocytes under simulated I/R. A more thorough investigation of p38 signaling is needed *in vitro* as well as *in vivo* following I/R before any conclusions can be drawn. While it is not known why PHLPP2 targets its substrates in certain cell types and under certain conditions, hopefully further studies in astrocytes will elucidate its mechanism of action.

Lastly, we also investigated the activation of Akt at Serine 473 following simulated I/R and after ROS stimulation in WT and PHLPP2 KO astrocytes. Although we found no significant difference in Akt Serine 473 phosphorylation between the WT and PHLPP2 KO brains under basal conditions, we found that phosphorylation was significantly increased with PHLPP2 removal in astrocytes following ischemia. In conditions that mimic ROS stimulation, removal of PHLPP2 did not accentuate Akt Serine 473 phosphorylation. This implies that the upregulation in Akt phosphorylation observed at reperfusion in the PHLPP2 KO astrocytes was probably mainly due to the significant upregulation in phosphorylation that occurred during ischemia alone. Since activation of Akt is known to promote pro-survival signaling in astrocytes and the brain (Chen et al. 2013), it is possible that upregulation of Akt observed during simulated ischemia in the PHLPP2 KO astrocytes was in response to damage, or removal of PHLPP2 may directly alter Akt phosphorylation only under stress. Future studies are needed to investigate Akt activity by activity assay as well as through analysis of the phosphorylation at Threonine 308, since phosphorylation of both residues are required for complete activation of Akt (Manning and Toker 2017). Also, phosphorylation of GSK3α/β, a downstream target of Akt, is indicative of Akt activity and

would further clarify our data (Mullonkal and Toledo-Pereyra 2007). If it is demonstrated that Akt activity is altered by PHLPP2 removal under ischemic conditions, WT and PHLPP2 KO astrocytes can be treated with an Akt inhibitor (Chen et al. 2013) to determine its role in inflammation and cell death of astrocytes exposed to simulated I/R.

Our laboratory previously found that PHLPP2 silencing via siRNA knock-down did not alter cell death levels in astrocytes following simulated ischemia compared to control (Chen et al. 2013). However, we found in the present study that astrocytes isolated from PHLPP2 KO mice potentiate cell death following simulated ischemia in culture compared to WT. This discrepancy could be attributed to the fact that the astrocytes in the PHLPP2 knock-down study had only undergone loss of PHLPP2 for two days prior to simulated ischemia (Chen et al. 2013), whereas in the present study, the astrocytes had loss of PHLPP2 since development. While our data suggests that during ischemia (2 hours) removal of PHLPP2 increases phosphorylation of Akt at Serine 473, and one would assume this would protect astrocytes from damage, this discrepancy could be attributed to the amount of time the astrocytes were exposed to ischemia. Following 18 hours of ischemia there may be alterations in Akt or pro-death pathways that could contribute to our finding. Future studies are needed in the PHLPP2 KO and WT astrocytes to determine whether apoptosis is significantly altered following simulated ischemia or if other pathways (i.e. necrosis and autophagy) may be involved. This would help to determine whether PHLPP2 removal truly does alter cell death of astrocytes or if the loss of PHLPP2 does not have a significant effect on apoptotic cell death, as was reported previously.

Future Studies

In conclusion, our study found that PHLPP2 removal might have detrimental consequences in astrocytes that have been exposed to conditions that mimic I/R. Specifically, we demonstrated that increased pro-death inflammatory signaling and MAP kinase signaling occurs, and that cell death levels increase upon removal of PHLPP2 in astrocytes under simulated I/R. These findings have implications for the usage of PHLPP as a pharmacological target. As previously mentioned, our laboratory demonstrated that PHLPP1 removal protects both astrocytes and neurons from injury in the brain caused by ischemic damage (Chen et al. 2013). Given our findings, it is suggested that PHLPP1 and PHLPP2 have opposing functions in astrocytes during I/R (Chen et al. 2013). Therefore, usage of pan-PHLPP inhibitors to treat victims of brain ischemia would not be an ideal usage of the PHLPP phosphatases as pharmacological targets. Two small molecule pan-PHLPP inhibitors (NSC117079 and NSC45586) were discovered by Sierecki and colleagues in 2010, and were then tested by Jackson and colleagues in 2013 in astrocytes (Sierecki et al. 2010; Jackson et al. 2013). Jackson and colleagues concluded that while specific inhibition of PHLPP1 accentuated Akt signaling in astrocytes, pan-PHLPP inhibition via usage of the inhibitors blocked pro-survival Akt activation in astrocytes and was overall detrimental (Jackson et al. 2013). Our findings agree with Jackson and colleagues' conclusion that developing an inhibitor specific to PHLPP1 would be a promising therapeutic to treat brain ischemia, rather than utilizing either of the currently available pan-PHLPP inhibitors. In addition to developing more specific PHLPP1 isoform inhibitors, future research is needed to determine the effects of overexpression of the PHLPP2 isoform on astrocyte function and signaling during simulated I/R. Investigating this could determine whether overexpression of PHLPP2 could be used as a therapeutic intervention to treat ischemic damage. Lastly, while the

changes with PHLPP2 removal have been investigated in astrocytes, using the PHLPP2 global KO mice we can examine the signaling in other cell types of the CNS, such as neurons and microglia, to further elucidate the effect of PHLPP2 removal on the CNS under conditions that mimic I/R. These studies would further clarify whether PHLPP1 and PHLPP2 have opposing or overlapping signaling in other cells of the CNS since this would be important in the context of therapeutic use following cerebral ischemia.

APPENDIX

Table 1: Hypoxia Media

Reagent	Source	Formula Weight (FW) or Stock Concentration	Quantity	Final Concentration
Sodium chloride	Fischer Scientific	5 M	14 mL	140 mM
Potassium chloride	Fischer Scientific	3 M	2 mL	12 mM
Magnesium chloride	Acros Organics	1 M	0.5 mL	1 mM
4-(2-hydroxyethyl)-1-piperazineethanesulfonic acid	Caisson Labs	1 M	5 mL	10 mM
Calcium chloride	Fischer Scientific	1 M	1 mL	2 mM

Add components to a glass beaker with 300 mL of water and stir. While stirring, pH the solution to 6.5. Add the solution to a graduated cylinder and fill to 500-mL mark with water. Filter sterilize the solution.

Table 2: Normoxia Media

Reagent	Source	FW or Stock Concentration	Quantity	Final Concentration
Sodium chloride	Fischer Scientific	5 M	14 mL	140 mM
Potassium chloride	Fischer Scientific	3 M	0.84 mL	5 mM
Magnesium chloride	Acros Organics	1 M	0.5 mL	1 mM
4-(2-hydroxyethyl)-1-piperazineethanesulfonic acid	Caisson Labs	1 M	5 mL	10 mM
Calcium chloride	Fischer Scientific	1 M	1 mL	2 mM
Glucose	Fischer Scientific	180	0.90 g	10 mM

Add components to a glass beaker with 300 mL of water and stir. While stirring, pH the solution to 7.4. Add the solution to a graduated cylinder and fill to 500-mL mark with water. Filter sterilize the solution.

Table 3: 0.5 M Ethylenediaminetetraacetic acid (EDTA)

Reagent	Source	FW or Stock Concentration	Quantity	Final Concentration
EDTA	Aldrich Chemical Company	372.24	93 g	0.5 M
Sodium hydroxide	Fischer Scientific	40	10 g	0.5 M

Combine components in approximately 300 mL of water. Stir and pH to 8. Add water such that total volume is 500 mL.

Table 4: RIPA Buffer (incomplete)

Reagent	Source	FW or Stock Concentration	Quantity	Final Concentration
Sodium chloride	Fischer Scientific	5 M	15 mL	150 mM
Tris (pH: 7.4)	Fischer Scientific	1 M	25 mL	50 mM
Nonidet P40 Substitute	USB Corporation	~603	5 mL	1%
Sodium deoxycholate	Alfa Aesar	432.58	5 g	23 mM
SDS	Hoefer	10%	5 mL	0.1%
EDTA	See Table 3	0.5 M	2 mL	2 mM
Sodium fluoride	Sigma-Aldrich	1 M	25 mL	50 mM

Combine components and add water such that total volume is 500 mL. Stir.

Table 5: 100 mM Phenylmethylsulfonyl fluoride

Reagent	Source	FW or Stock Concentration	Quantity	Final Concentration
Phenylmethylsulfonyl fluoride	Calbiochem	174.2	1.4 g	100 mM
Isopropanol	Fischer Scientific	60.1	80 mL	N/A

Combine components.

Table 6: RIPA Buffer

Reagent	Source	FW or Stock Concentration	Quantity	Final Concentration
RIPA Buffer (incomplete)	See Table 4	15.4%	5 mL	15.1%
para-Nitrophenylphosphate	Sigma-Aldrich	1 M	5 µL	1 mM
Sodium orthovanadate (pH: 10)	Fischer Scientific	500 mM	5 µL	0.5 mM
Leupeptin	Fischer Scientific	10 mg/mL	5 µL	10 µg/mL
Aprotinin	Sigma-Aldrich	200X	33 µL	1X
Phenylmethylsulfonyl fluoride	See Table 5	100 mM	50 µL	1 mM

Vortex sodium orthovanadate and phenylmethylsulfonyl fluoride prior to use. Combine components and mix.

Table 7: 5X SDS Loading Dye

Reagent	Source	FW or Stock Concentration	Quantity	Final Concentration
Tris (pH: 7)	Fischer Scientific	1 M	12 mL	0.25 M
Glycerol	Fischer Scientific	92.09	19.2 mL	40%
SDS	Hoefer	288.38	3.84 g	277 mM
β-Mercaptoethanol	Sigma-Aldrich	78.13	9.6 mL	20%
Bromophenol blue	Fischer Scientific	669.96	0.048 g	.0015 mM

Combine the components and add water such that the total volume is 48 mL.

Table 8: MOPS Buffer

Reagent	Source	FW or Stock Concentration	Quantity	Final Concentration
MOPS	Spectrum Chemical	209.26	836.8 g	1 M
Tris-base	Gentrox	121.14	484.8 g	1 M
SDS	Hoefer	288.38	80 g	69.4 mM
EDTA	Aldrich Chemical Company	372.24	24 g	16.1 mM

Dissolve components in 2 L of water. Add more water such that the total volume is 4 L. Dilute with water in a 1:20 ratio for 1X MOPS Buffer.

Table 9: TA Buffer

Reagent	Source	FW or Stock Concentration	Quantity	Final Concentration
TA Buffer	Novex Life Technologies	20X	50 mL	1X

Dissolve in 950 mL of water.

Table 10: 20X Transfer Buffer

Reagent	Source	FW or Stock Concentration	Quantity	Final Concentration
Tris-base	Gentrox	121.14	145.6 g	0.24 M
Glycine	Gentrox	75.07	720 g	1.92 M

Combine components in 2 L of water. Add water such that the total volume is 5 L.

Table 11: 1X Transfer Buffer

Reagent	Source	FW or Stock Concentration	Quantity	Final Concentration
20X Transfer Buffer	See Table 10	20X	50 mL	1X
Methanol	Fischer Scientific	32.04 g/mol	200 mL	20%

Combine components and add water such that the total volume is 1 L.

Table 12: 10X TBS

Reagent	Source	FW or Stock Concentration	Quantity	Final Concentration
Tris hydrochloride	Fischer Scientific	157.6	63 g	0.1 M
Sodium chloride	Fischer Scientific	58.44 g/mol	70.2 g	0.3 M

Combine components in 2 L of water. pH to 7.5. Add water such that the total volume is 4 L.

Table 13: 0.1% TBS-T

Reagent	Source	FW or Stock Concentration	Quantity	Final Concentration
10X TBS	See Table 12	10X	2 L	10%
Tween-20	Chem-Impex International	1227.54	20 mL	0.1 %

Combine components and add water such that the total volume is 20 L.

Table 14: Western Blot Antibody List

Antigen	Product Source/ Catalog #	Dilution	Source
PHLPP2 (primary)	Bethyl #A300-661A	1:2000	Rabbit
PHLPP1β (primary)	Bethyl #A300-660A	1:2000	Rabbit
GAPDH (primary)	Cell Signaling Technology #2118	1:1000	Rabbit
Phosphorylated Akt (Ser473) (primary)	Cell Signaling Technology #9271	1:1000	Rabbit
Phosphorylated GSK3α/β (Ser21/9) (primary)	Cell Signaling Technology #9331	1:1000	Rabbit
Phosphorylated ERK1/2 (Thr202/Tyr204) (primary)	Cell Signaling Technology #9101	1:1000	Rabbit
Phosphorylated p70S6K (Thr389) (primary)	Cell Signaling Technology #9234	1:1000	Rabbit
Phosphorylated p65 (Ser536) (primary)	Cell Signaling Technology #3033	1:1000	Rabbit

Table 14: Western Blot Antibody List (continued)

Antigen	Product Source/ Catalog #	Dilution	Source
Phosphorylated JNK (Thr183/Tyr185) (primary)	Cell Signaling Technology #4668	1:1000	Rabbit
Phosphorylated p38 (Thr180/Tyr182) (primary)	Cell Signaling Technology #4511	1:1000	Rabbit
β-actin (primary)	Cell Signaling Technology #8457	1:1000	Rabbit
α-tubulin (primary)	Cell Signaling Technology #2144	1:1000	Rabbit
Anti-Rabbit Immunoglobin G (secondary)	Sigma-Aldrich #A6154	1:8000	N/A

Table 15: cDNA Synthesis Mix

Reagent	Source	FW or Stock Concentration	Quantity	Final Concentration
10X RT Random Primers	Fischer Scientific	10X	2 µL	20%
dNTP Mix	Fischer Scientific	100 mM	0.8 µL	8%
RNAse Inhibitor	Fischer Scientific	20 units/µL	1 µL	10%
MultiScribe Reverse Transcriptase	Fischer Scientific	50 units/µL	1 µL	10%
10X RT Buffer	Fischer Scientific	10X	2 µL	20%

Combine the components with 3.2 µL of sterile water. Add to 1 µg RNA (10 µL volume), for a final volume of 20 µL.

Table 16: RT-PCR Protocol

Time	Temperature
10:00	25 °C
2:00:00	37 °C
5:00	85 °C
Hold	4 °C

Table 17: qPCR Primer List

Gene of Interest (Mouse)	Integrated DNA Technologies #
GAPDH	Mm.PT.39a.1
IL1B	Mm.PT.58.41616450
IL6	Mm.PT.58.10005566
TNF**α**	Mm.PT.58.12575861
COX-2	Mm.PT.58.9154407
NLRP3	Mm.PT.58.13974318

Table 18: qPCR Protocol

Stage	Time	Temperature
Holding	2:00	50°C
Holding	10:00	95°C
Cycling	0:15	95°C
Cycling	1:00	60°C

Following cDNA synthesis, dilute each reaction by adding 20 µL of sterile water (40 µL total). Dilute cDNA again by adding sterile water (1:25 dilution). Add 9 µL of diluted cDNA to 1 µL of primer (see Table 17) and 10 µL of qPCRBIO Probe Mix Lo-Rox (Genesee Scientific), and add to the wells of a 96-well qPCR plate. Run the plate on 7500 fast StepOne Real-Time PCR System (Thermo Scientific). Cycling stage repeats 40 times. Analyze relative quantification using the comparative threshold cycle (Ct) method normalized to glyceraldehyde 3-phosphate dehydrogenase (GAPDH) as described previously (Schmittgen and Livak 2008).

Table 19: 1X JNK Lysis Buffer (incomplete)

Reagent	Source	FW or Stock Concentration	Quantity	Final Concentration
Tris (pH: 7.6)	Fischer Scientific	1 M	10 mL	20 mM
Sodium chloride	Fischer Scientific	5 M	25 mL	250 mM
EDTA	See Table 3	0.5 M	3 mL	3 mM
Egtazic acid	Sigma-Aldrich	0.1 M	15 mL	3 mM
β-glycero-phosphate (pH: 7.6)	Sigma-Aldrich	1 M	10 mL	20 mM
Nonidet P40 Substitute	USB Corporation	~603	2.5 mL	0.5%

Combine components and add water such that the total volume is 500 mL. Filter sterilize the solution.

Table 20: JNK Lysis Buffer

Reagent	Source	FW or Stock Concentration	Quantity	Final Concentration
JNK Lysis Buffer (incomplete)	See Table 18	1X	5 mL	98%
para-Nitrophenylphosphate	Sigma-Aldrich	1 M	5 µL	1 mM
Sodium orthovanadate (pH: 10)	Fischer Scientific	500 mM	5 µL	0.5 mM
Leupeptin	Fischer Scientific	10 mg/mL	5 µL	10 µg/mL
Aprotinin	Sigma-Aldrich	200X	33 µL	1X
Phenylmethylsulfonyl fluoride	See Table 5	100 mM	50 µL	1 mM

Vortex sodium orthovanadate and phenylmethylsulfonyl fluoride prior to use. Combine components and mix.

Table 21: Western Buffer

Reagent	Source	FW or Stock Concentration	Quantity	Final Concentration
Sodium phosphate (pH: 7)	Sigma Aldrich	0.5 M	20 mL	20 mM
Sodium chloride	Fischer Scientific	5 M	15 mL	150 mM
Magnesium chloride	Acros Organics	1 M	1 mL	2 mM
Nonidet P40	Sigma Aldrich	100%	0.5 mL	0.1%
Glycerol	Fisher Scientific	100%	50 mL	10%
Okadaic acid	Sigma Aldrich	10 µM	0.5 mL	10 nM
Sodium fluoride	Sigma Aldrich	1 M	5 mL	10 mM
Sodium pyrophosphate	Sigma Aldrich	0.5 M	10 mL	10 mM
Dithiothreitol	Sigma Aldrich	1 M	0.5 mL	1 mM
Sodium orthovanadate	Sigma Aldrich	200 mM	0.0092 g	0.1 mM
Pepstatin	Sigma Aldrich	1 mg/mL	5 mL	10 µg/mL
Leupeptin	Sigma Aldrich	1 mg/mL	5 mL	10 µg/mL
Aprotinin	Sigma Aldrich	25 mg/mL	200 µL	10 µg/mL

Table 21: Western Buffer (continued)

Reagent	Source	FW or Stock Concentration	Quantity	Final Concentration
N_{α}-Tosyl-L-lysine chloromethyl ketone hydrochloride	Sigma Aldrich	5 mg/mL	1 mL	10 μg/mL
L-1-Tosylamide-2-phenylethyl chloromethyl ketone	Sigma Aldrich	5 mg/mL	1 mL	10 μg/mL

Add components to 250 mL of water, then bring up the volume to 500 mL and stir.

REFERENCES

Agarwal, Nitin Kumar, Xiaoping Zhu, Mihai Gagea, Charles L. White III, Gilbert Cote, and Maria-Magdalena Georgescu. "PHLPP2 Suppresses the NF-KB Pathway by Inactivating IKKβ Kinase." *Oncotarget*, vol. 5, no. 3, Feb. 2014, pp. 815–823. *PubMed Central*, doi:10.18632%2Foncotarget.1774.

Aharon, A. S., M. R. Mulloy, D. C. Drinkwater Jr., O. B. Lao, M. D. Johnson, M. Thunder, C. Yu, and P. Chang. "Cerebral Activation of Mitogen-Activated Protein Kinases after Circulatory Arrest and Low Flow Cardiopulmonary Bypass." *European Journal of Cardio-thoracic Surgery*, vol. 26, no. 5, Nov. 2004. *PubMed Central*, doi: 10.1016/j.ejcts.2004.05.040.

Barone, F. C., E. A. Irving, A. M. Ray, J. C. Lee, S. Kassis, S. Kumar, A. M. Badger, R. F. White, M. J. McVey, J. J. Legos, J. A. Erhardt, A. H. Nelson, E. H. Ohlstein, A. J. Hunter, K. Ward, B. R. Smith, J. L. Adams, and A. A. Parsons. "SB 239063, a Second-Generation p38 Mitogen-Activated Protein Kinase Inhibitor, Reduces Brain Injury and Neurological Deficits in Cerebral Focal Ischemia." *The Journal of Pharmacology and Experimental Therapeutics*, vol. 296, no. 2, Feb. 2001, pp. 312–321., jpet.aspetjournals.org/content/296/2/312.long.

Barreto, George, Robin E. White, Yibing Ouyang, Lijun Xu, and Rona G. Giffard. "Astrocytes: Targets for Neuroprotection in Stroke." *Central Nervous System Agents in Medicinal Chemistry*, vol. 11, no. 2, 1 June 2011, pp. 164–173. *PubMed Central*, doi:10.2174/187152411796011303.

Brognard, John, Emma Sierecki, Tianyan Gao, and Alexandra C. Newton. "PHLPP and a Second Isoform, PHLPP2, Differentially Attenuate the Amplitude of Akt Signaling by Regulating Distinct Akt Isoforms." *Molecular Cell*, vol. 25, no. 6, 23 Mar. 2007, pp. 917–931. *ScienceDirect*, doi:10.1016/j.molcel.2007.02.017.

Chen, Bo, Jessica A. Van Winkle, Patrick D. Lyden, Joan H. Brown, and Nicole H. Purcell. "PHLPP1 Gene Deletion Protects the Brain from Ischemic Injury." *Journal of Cerebral Blood Flow & Metabolism*, vol. 33, no. 2, Feb. 2013, pp. 196–204. *PubMed Central*, doi:10.1038/jcbfm.2012.150.

Cho, Deog-Gon, Matthew R. Mulloy, Paul A. Chang, Mahlon D. Johnson, Alon S. Aharon, Trevor A. Robison, Tamara L. Buckles, Daniel W. Byrne, and Davis C. Drinkwater Jr. "Blockade of the Extracellular Signal-Regulated Kinase Pathway by UO126 Attenuates Neuronal Damage Following Circulatory Arrest." *The Journal of Thoracic and Cardiovascular Surgery*, vol. 127, no. 4, Apr. 2004, pp. 1033-1040. doi: 10.1016/j.jtcvs.2003.09.038.

Citro, Simona, Sundeep Malik, Emily A. Oestreich, Julie Radeff-Huang, Grant G. Kelley, Alan V. Smrcka, and Joan Heller Brown. "Phospholipase C Is a Nexus for Rho and Rap-Mediated G Protein-Coupled Receptor-Induced Astrocyte Proliferation." *Proceedings of the National Academy of Sciences of the United States of America*, vol. 104, no. 39, 25 Sept. 2007, pp. 15543–15548. *PubMed Central*, doi:10.1073/pnas.0702943104.

Clarke, Laura E., Shane A. Liddelow, Chandrani Chakraborty, Alexandra E. Munch, Myriam Heiman, and Ben A. Barres. "Normal Aging Induces A1-Like Astrocyte Reactivity." *Proceedings of the National Academy of Sciences of the United States of America*, vol. 115, no. 8, 20 Feb. 2018, pp. E1896–E1905., doi:10.1073/pnas.1800165115.

Doll, Danielle N., Taura L. Barr, and James W. Simpkins. "Cytokines: Their Role in Stroke and Potential Use as Biomarkers and Therapeutic Targets." *Aging and Disease*, vol. 5, no. 5, 1 Oct. 2014, pp. 294–306. *PubMed Central*, doi:10.14336/ad.2014.0500294.

Font-Nieves, Miriam, M. Gloria Sans-Fons, Roser Gorina, Ester Bonfill-Teixidor, Angelica Salas-Perdomo, Leonardo Marquez-Kisinousky, Tomas Santalucia, and Anna M. Planas. "Induction of COX-2 Enzyme and Down-Regulation of COX-1 Expression by Lipopolysaccharide (LPS) Control Prostaglandin E2 Production in Astrocytes." *Journal of Biological Chemistry*, vol. 287, no. 9, 24 Feb. 2012, pp. 6454–6468. *PubMed Central*, doi:10.1074/jbc.m111.327874.

Gao, Tianyan, Frank Furnari, and Alexandra C. Newton. "PHLPP: A Phosphatase That Directly Dephosphorylates Akt, Promotes Apoptosis, and Suppresses Tumor Growth." *Molecular Cell*, vol. 18, no. 1, 1 Apr. 2005, pp. 13–24. *ScienceDirect*, doi:10.1016/j.molcel.2005.03.008.

Granger, D. Neil, and Peter R. Kvietys. "Reperfusion Injury and Reactive Oxygen Species: The Evolution of a Concept." *Redox Biology*, vol. 6, Dec. 2015, pp. 524–551. *PubMed Central*, doi:10.1016/j.redox.2015.08.020.

Grzechnik, A. T., and A. C. Newton. "PHLPPing through History: a Decade in the Life of PHLPP Phosphatases." *Biochemical Society Transactions*, vol. 44, no. 6, 15 Dec. 2016, pp. 1675–1682. *PubMed Central*, doi:10.1042/bst20160170.

Guha, Mausumee, Maria A. O'Connell, Rafal Pawlinkski, Angela Hollis, Patricia McGovern, Shi-Fang Yan, David Stern, and Nigel Mackman. "Lipopolysaccharide Activation of the MEK-ERK1/2 Pathway in Human Monocytic Cells Mediates Tissue Factor and Tumor Necrosis Factor **α** Expression by Inducing Elk-1 Phosphorylation and Egr-1 Expression." *Blood*, vol. 98, no. 5, 1 Sept. 2001, 1429-1439. doi: 10.1182/blood.V98.5.1429

He, Yuan, Hideki Hara, and Gabriel Nunez. "Mechanism and Regulation of NLRP3 Inflammasome Activation." *Trends in Biochemical Sciences*, vol. 41, no. 12, Dec. 2016. *Cell*, doi:10.1016/j.tibs.2016.09.002

Irving, Elaine A., and Mark Bamford. “Role of Mitogen- and Stress-Activated Kinases in Ischemic Injury.” *Journal of Cerebral Blood Flow & Metabolism*, vol. 22, no. 6, 2002, pp. 631–647. *SAGE Journals*, doi:10.1097/00004647-200206000-00001.

Jackson, T. C., Jonathan D. Verrier, Tomas Drabek, Keri Janesko-Feldman, Delbert G. Gillespie, Thomas Uray, Cameron Dezfulian, Robert S. Clark, Hulya Bayir, Edwin K. Jackson, and Patrick M. Kochanek. “Pharmacological Inhibition of Pleckstrin Homology Domain Leucine-Rich Repeat Protein Phosphatase Is Neuroprotective: Differential Effects on Astrocytes.” *Journal of Pharmacology and Experimental Therapeutics*, vol. 347, no. 2, Nov. 2013, pp. 516–528. *PubMed Central*, doi:10.1124/jpet.113.206888.

Jakel, Sarah, and Leda Dimou. “Glial Cells and their Function in the Adult Brain: a Journey through the History of their Ablation.” *Frontiers in Cellular Neuroscience*, vol. 11, no. 24, 2017. *PubMed Central*, doi:10.3389fncel.2017.00024.

Kawabori, Masahito, and Midori A. Yenari. “Inflammatory Responses in Brain Ischemia.” *Current Medicinal Chemistry*, vol. 22, no. 10, 2015, pp. 1258–1277. *PubMed Central*, doi:10.2174/0929867322666150209154036.

Kawasome, Hideki, Philip Papst, Saiphone Webb, Gordon M. Keller, Gary L. Johnson, Erwin W. Gelfand, and Naohiro Terada. “Targeted Disruption of p70s6k Defines Its Role in Protein Synthesis and Rapamycin Sensitivity.” *Proceedings of the National Academy of Sciences of the United States of America*, vol. 95, no. 9, 28 Apr. 1998, pp. 5033–5038. *PubMed Central*, doi:10.1073/pnas.95.9.5033.

Kim, Min-Ji, Joo-Heon Yoon, and Ji-Hwan Ryu. “Mitophagy: a Balance Regulator of NLRP3 Inflammasome Activation.” *Korean Society for Biochemistry and Molecular Biology Reports*, vol. 49, no. 10, 31 Oct. 2016, pp. 529–535. *PubMed Central*, doi:10.5483/bmbrep.2016.49.10.115.

Lamkanfi, Mohamed, R. K. Subbarao Malireddi, and Thirumala-Devi Kanneganti. “Fungal Zymosan and Mannan Activate the Cryopyrin Inflammasome.” *Journal of Biological Chemistry*, vol. 284, no. 31, 31 July 2009, pp. 20574–20581. *PubMed Central*, doi:10.1074/jbc.m109.023689.

Lee, Gilbert Aaron, Yein-Gei Lai, Ray-Jade Chen, and Nan-Shih Liao. “Interleukin 15 Activates Akt to Protect Astrocytes from Oxygen Glucose Deprivation-Induced Cell Death.” *Cytokine*, vol. 92, Apr. 2017, pp. 68–74. *ScienceDirect*, doi:10.1016/j.cyto.2017.01.010.

Li, Xin, Payton D. Stevens, Jianyu Liu, Haihua Yang, Wei Wang, Chi Wang, Zheng Zeng, Michael D. Schmidt, Mike Yang, Eun Y. Lee, and Tianyan Gao. “PHLPP Is a Negative Regulator of RAF1, Which Reduces Colorectal Cancer Cell Motility and Prevents Tumor Progression in Mice.” *Gastroenterology*, vol. 146, no. 5, May 2014, pp. 1301–1312. *PubMed Central*, doi:10.1053/j.gastro.2014.02.003.

Libermann, T. A., and D. Baltimore. “Activation of Interleukin-6 Gene Expression through the NF-Kappa B Transcription Factor.” *Molecular and Cellular Biology*, vol. 10, no. 5, May 1990, pp. 2327–2334. *PubMed Central*, doi:10.1128/mcb.10.5.2327.

Liddelow, Shane A., and Ben A. Barres. “Reactive Astrocytes: Production, Function, and Therapeutic Potential.” *Immunity*, vol. 46, no. 6, 2017, pp. 957–967. *ScienceDirect*, doi:10.1016/j.immuni.2017.06.006.

Lim, Joo Weon, Hyeyoung Kim, and Kyung Hwan Kim. “Nuclear Factor-KB Regulates Cyclooxygenase-2 Expression and Cell Proliferation in Human Gastric Cancer Cells.” *Laboratory Investigation*, vol. 81, no. 3, Mar. 2001, pp. 349–360. *PubMed Central*, doi:10.1038/labinvest.3780243.

Liu, Jianyu, Payton D. Stevens, Xin Li, Michael D. Schmidt, and Tianyan Gao. “PHLPP-Mediated Dephosphorylation of S6K1 Inhibits Protein Translation and Cell Growth.” *Molecular and Cellular Biology*, 23 Nov. 2011, doi:10.1128/mcb.05799-11.

Manning, Brendan D. and Alex Toker. “Akt/PKB Signaling: Navigating the Network.” *Cell*, vol. 169, no. 3, 20 Apr. 2017, pp. 381-405. *PubMed Central*, doi:10.1016/j.cell.2017.04.001.

Mullonkal, Carolyn J., and Luis H. Toledo-Pereyra. “Akt in Ischemia and Reperfusion.” *Journal of Investigative Surgery*, vol. 20, no. 3, 2007, pp. 195–203. *Taylor & Francis Online*, doi:10.1080/08941930701366471.

Møller, Michael B. “p27 In Cell Cycle Control and Cancer.” *Leukemia & Lymphoma*, vol. 39, no. 1-2, 2000, pp. 19–27. *Taylor and Francis Online*, doi:10.3109/10428190009053535.

Qiao, Meng, Yaqi Wang, Xiaoen Xu, Jing Lu, Yongli Dong, Wufan Tao, Janet Stein, Gary S. Stein, James D. Iglehart, Qian Shi, and Arthur B. Pardee. “Mst1 Is an Interacting Protein That Mediates PHLPPs' Induced Apoptosis.” *Molecular Cell*, vol. 38, no. 4, 28 May 2010, pp. 512–523. *ScienceDirect*, doi:10.1016/j.molcel.2010.03.017.

Qiao, Yu, Peng Wang, Jianni Qi, Lei Zhang, and Chengjiang Gao. “TLR-Induced NF-KB Activation Regulates NLRP3 Expression in Murine Macrophages.” *Federation of European Biochemical Societies Letters*, vol. 586, no. 7, 8 Mar. 2012, pp. 1022–1026. *Wiley Online Library*, doi:10.1016/j.febslet.2012.02.045.

Rossol, M., H. Heine, U. Meusch, D. Quandt, C. Klein, M. J. Sweet, and S. Hauschildt. “LPS-Induced Cytokine Production in Human Monocytes and Macrophages.” *Critical Reviews in Immunology*, vol. 31, no. 5, 2011, pp. 379–446. *PubMed Central*, doi:10.1615/critrevimmunol.v31.i5.20.

Saggu, Raman, Toni Schumacher, Florian Gerich, Cordula Rakers, Khalid Tai, Andrea Delekate, and Gabor C. Petzold. "Astroglial NF-κB Contributes to White Matter Damage and Cognitive Impairment in a Mouse Model of Vascular Dementia." *Acta Neuropathologica Communications*, vol. 76, no. 4, 4 Aug. 2016., doi:10.1186/s40478-016-0350-3.

Saud, K., R. Herrera-Molina, and R. Von Bernhardi. "Pro- and Anti-Inflammatory Cytokines Regulate the ERK Pathway: Implication of the Timing for the Activation of Microglial Cells." *Neurotoxicity Research*, vol. 3, no. 3-4, Nov. 2005, pp. 277-287. *PubMed Central*.

Schmittgen, Thomas D, and Kenneth J Livak. "Analyzing Real-Time PCR Data by the Comparative CT Method." *Nature Protocols*, vol. 3, no. 6, 5 June 2008, pp. 1101–1108., doi:10.1038/nprot.2008.73.

Shi, Y., F. Nikulenkov, J. Zawacka-Pankau, H. Li, R. Gabdoulline, J. Xu, S. Eriksson, E. Hedstrom, N. Issaeva, A. Kel, E. S. J. Arner, and G. Selivanova. "ROS-Dependent Activation of JNK Converts p53 into an Efficient Inhibitor of Oncogenes Leading to Robust Apoptosis." *Cell Death & Differentiation*, vol. 21, 10 Jan. 2014, pp. 612-623., doi:10.1038/cdd.2013.186

Shimizu, Kimiko, Scott M. Mackenzie, and Daniel R. Storm. "SCOP/PHLPP and its Functional Role in the Brain." *Molecular BioSystems*, vol. 6, no. 1, Jan. 2010, pp. 38-43. *PubMed Central*, doi:10.1039/b911410f.

Sierecki, Emma, William Sinko, J. Andrew McCammon, and Alexandra C. Newton. "Discovery of Small Molecule Inhibitors of the PH Domain Leucine-Rich Repeat Protein Phosphatase (PHLPP) by Chemical and Virtual Screening." *Journal of Medicinal Chemistry*, vol. 53, no. 19, 14 Oct. 2010, pp. 6899–6911. *PubMed Central*, doi:10.1021/jm100331d.

Sofroniew, Michael V., and Harry V. Vinters. "Astrocytes: Biology and Pathology." *Acta Neuropathologica*, vol. 119, no. 1, Jan. 2010, pp. 7–35. *PubMed Central*, doi:10.1007/s00401-009-0619-8.

"Stroke Information." *Centers for Disease Control and Prevention*, 13 Feb. 2019, www.cdc.gov/stroke/index.htm.

Sugino, Toshiyuki, Kazuhiko Nozaki, Yasushi Takagi, Itaro Hattori, Nobuo Hashimoto, Tetsuo Moriguchi, and Eisuke Nishida. "Activation of Mitogen-Activated Protein Kinases after Transient Forebrain Ischemia in Gerbil Hippocampus." *The Journal of Neuroscience*, vol. 20, no. 12, 15 June 2000, pp. 4506–4514., doi:10.1523/jneurosci.20-12-04506.2000.

Szydlowska, Kinga, Agata Gozdz, Michal Dabrowski, Malgorzata Zawadzka, and Bozena Kaminska. “Prolonged Activation of ERK Triggers Glutamate-Induced Apoptosis of Astrocytes: Neuroprotective Effect of FK506.” *Journal of Neurochemistry*, vol. 113, no. 4, 14 Apr. 2010, pp. 904–918. *Wiley Online Library*, doi:10.1111/j.1471-4159.2010.06656.x.

Teng, D. C., J. Sun, Y. Q. An, Z. H. Hu, P. Liu, Y. C. Ma, B. Han, and Y. Shi. “Role of PHLPP1 in Inflammation Response: Its Loss Contributes to Gliomas Development and Progression.” *International Immunopharmacology*, vol. 34, May 2016, pp. 229–234. *PubMed Central*, doi:10.1016/j.intimp.2016.02.034.

Wang, Z. Q., D. C. Wu, F. P. Huang, and G. Y. Yang. “Inhibition of MEK/ERK 1/2 Pathway Reduces Pro-Inflammatory Cytokine Interleukin-1 Expression in Focal Cerebral Ischemia.” *Brain Research*, vol. 996, no. 1, 16 Jan. 2004, pp. 55–66. *PubMed Central*, doi:10.1016/j.brainres.2003.09.074.

Wei, Xiu-E, Feng-Yu Zhang, Kai Wang, Qing-Xiu Zhang, and Liang-Qun Rong. “Assembly of the FKBP51-PHLPP2-AKT Signaling Complex in Cerebral Ischemia/Reperfusion Injury in Rats.” *Brain Research*, vol. 1566, 30 May 2014, pp. 60–68. *ScienceDirect*, doi:10.1016/j.brainres.2014.04.009.

Welsh, G. I., and C. G. Proud. “Glycogen Synthase Kinase-3 Is Rapidly Inactivated in Response to Insulin and Phosphorylates Eukaryotic Initiation Factor EIF-2B.” *Biochemical Journal*, vol. 294, no. 3, 15 Sept. 1993, pp. 625–629. *PubMed Central*, doi:10.1042/bj2940625.

Zhu, Junlan, Jingjie Zhang, Haishan Huang, Jingxia Li, Yonghui Yu, Honglei Jin, Yang Li, Xu Deng, Jimin Gao, Qinshi Zhao, and Chuanshu Huang. “Crucial Role of c-Jun Phosphorylation at Ser63/73 Mediated by PHLPP Protein Degradation in the Cheliensisin A Inhibition of Cell Transformation.” *Cancer Prevention Research*, vol. 7, no. 12, Dec. 2014, doi:10.1158/1940-6207.CAPR-14-0233.